Montanuniversität Leoben

Preheating of austenitic stainless steel for cold forming

Masterarbeit

Florian Zielbauer

Die vorliegende Arbeit wurde am Department Metallkunde und Werkstoffprüfung der Montanuniversität Leoben in Kooperation mit Hilti AG durchgeführt.

Leoben, 05.09.2018

Eidesstattliche Erklärung

Ich erkläre an Eides statt, dass ich diese Arbeit selbstständig verfasst, andere als die angegebenen Quellen und Hilfsmittel nicht benutzt und mich auch sonst keiner unerlaubten Hilfsmittel bedient habe.

Affidavit

I declare in lieu of oath, that I wrote this thesis and performed the associated research myself, using only literature cited in this volume.

Leoben, Datum _____

II. Table of content

III. Acknowledgements

My sincere appreciation to my supervisors Ronald Schnitzer and Rohr Jürgen for their guidance and encouragement over the last months, for all the knowledge they were able to impart to me and for supporting me in every way.

I would like to express my gratitude to the anchors unit of Plant 1 for helping me with finishing my project giving me all the necessary assistance.

Many special thanks to all my colleagues of the engineering department of the anchors unit in Plant 1 for all the good advices and for the great working atmosphere. I really enjoyed working with all of you!

Special thanks to Stefan Fabbro, who never stopped supporting me with my thesis and helped with constructive advices and motivating words when needed, to Thomas Zauchner for being a friend through all these years and for helping me out in every situation and to Florian Kusztrits, who especially in the last months walked this difficult path together with me motivating and supporting in every way necessary.

My deepest appreciation to all my friends who remain unnamed for always being their when needed and bringing me through some rough times. Thank you for all the good memories, you made these years of study unforgettable.

I would like to thank my parents, my siblings and my grandparents not only for the financial support, also for their continuous love, for believing in me even in hard times and encouraging me whenever I needed it the most. Thank you for being there and giving me the feeling of safety.

Moreover, I want to express my thanks to my fiancée's family for accepting me without consequences into their family. Thank you for always welcoming me in your caring home and treating me like one of your own.

Furthermore, a big thank you to my long-time friends of Pesendorf for bringing me back to normality in chaotic times and familiarity whenever I visited home. Thank you for never changing the way we are.

Finally and most importantly, I want to express my deepest gratitude to my fiancée Julia for her never ending support and ability to calm me down in every situation. Thank you for your endless patience and strong believe in me when I doubted myself the most. Thank you for the past five years.

IV. Abstract

To outperform competition in the market of metal anchors it is crucial to keep the product quality as high as possible and the price as low as necessary. Although the process of cold forming is well established, there is still optimization potential. In order to rise the performance and load limit of the anchors, different geometries in combination with high-strength steels are necessary. As a result, the machines, the forming and rolling dies suffer higher wear, which leads to high production costs.

To get a rough idea of the flow properties in advance, crush tests on wire-samples had been done. With a better understanding of the flow behavior of different materials and therefore better possibilities of doing an improved computer-aided simulation previously, tests at the - cold former can be defined more preciously and efficient.

As expected the flow properties of the tested material 1.4404 improve with increasing temperature of the sample. The ideal preheating temperature for this material seems to be 300° C. No significant change in flow properties were detected between 300° C and 400° C and over 400° C the possibility of forming carbides in the microstructure is too high, which would negatively impact the corrosion resistance of the material.

Looking for methods to increase the lifetime of the components in the cold former, preheating of the wire seems to be an appropriate solution. With better flow properties and less strength of the material at higher temperatures the tool wear could be decreased.

To verify this assumption, tests have been planned on cold former which is already used for the metal anchor production. In order to heat the wire before the forming process an inductor operated by a generator was mounted in the cold former.

Due to the fact, that the power of the used generator was not high enough, 300° C could not be reached. The maximum temperature reached with the testing setup was around 150° C, which had no positive influence on the forming force. Nevertheless, small improvements at the thread rolling process, according to geometry and decrease of forces were determined.

V. Kurzfassung

Starker Konkurrenzkampf am Metallankermarkt zwingt Firmen ihre Produkte qualitativ immer besser und preislich günstiger auf den Markt zu bringen, um sich gegen die grosse Anzahl an Mitbewerbern behaupten zu können. Obwohl der Prozess des Kaltumformens seit Jahrzehnten im Bereich der Dübelfertigung etabliert ist, gibt es immer noch ausreichend Verbesserungspotential. Auch bei den Produkten versucht man durch komplexere Geometrien und höherfeste Stähle höhere Lastwerte und bessere Performance zu erreichen. Dadurch kommt es zu erheblichen Verschleiss an Werkzeug und Maschine, welches sich direkt auf die Produktionskosten niederschlägt.

Um im Vorfeld eine Aussage über das Verformungs- und Fliessverhalten eines Werkstoffes treffen zu können, kommen unter anderem Stauchtests zur Anwendung. Mit derartigen Tests kann ein besseres Verständnis für den Werkstoff und dessen Eigenschaften erlangt werden. In weiterer Folge können dadurch computerbasierte Simulationen optimiert werden.

Wie erwartet wurde das Fliessverhalten des getesteten Werkstoffes, 1.4404, mit steigender Temperatur besser. Als Temperatur für spätere Versuche wurden 300° C definiert, da zwischen 300° C und 400° C keine grosse Kraftreduktion festgestellt werden konnten und die Gefahr der Karbidbildung, welche sich negativ auf das Korrosionsverhalten auswirken würde, ab 400° C zu gross ist.

Als eine Methode um den Werkzeugverschleiss in den Kaltumformern zu minimieren schien sich Vorwärmen des Drahtes anzubieten. Durch verbessertes Fliessverhalten des Drahtes und eine Kraftminimierung beim Umformprozess könnte möglicherweise die Standzeit der Umformmatrizen und Stempel verlängert und so die Kosten bei der Produktion reduziert werden.

Um dies zu realisieren wurde ein Induktor in den Umformer integriert. Aufgrund des zu schwachen Generators konnte die gewünschte Temperatur nicht erreicht werden, daher war es nicht möglich eine Aussage über die Kraftreduktion treffen zu können. Es wurde ein minimaler Anstieg der Kraft mit steigender Temperatur vermerkt. Geringe Verbesserungen im Bereich der Geometrie und Walzkraft konnten beim Gewindewalzen beobachtet werden.

VI. Abbreviations and used symbols

HPASS ..... High Performance Austenitic Stainless Steel

AOD ..... Organ-Oxygen-Decarburization

VOD..... Vacuum-Oxygen-Decarburization

TTT ..... Time-Temperature-Transformation

σ ..... Tension

ε ..... Elongation

φ ..... Forming Speed

AISI..... American Iron and Steel Institute

IBC..... Intermediate Bulk Container

°C ..... Degree Celsius

°F..... Degree Fahrenheit

1. Motivation

In order to allow higher loads and better performance of screw and stud anchors, different and more complex geometries in combination with the use of high strength steels is inevitable. The constant competition on the market needs constant improvement of cold forming processes and needs them to operate on a very high technical level. Next to a steady improvement of forming concepts and forming tools, which increases the lifetime and therefore reduces production costs, the concept of preheating before the forming process presents itself as an interesting optimization. The idea behind the preheating process is to lower the forces of the forming process by decreasing the yield strength of the material. Tool wear and therefore the production costs might be decreased as a consequence. Another aspect is the improvement of the flow properties by rising temperatures in the material. This could lead to the possibility of realising more complex component geometries which probably will lead to a better performance of the products.

Fewer tool failures leads automatically to less machine downtime, which results in lower production costs. An aspect is the increase of the lifetime of the whole cold former. The constant production at the limit of the cold former's technical capabilities leads to a higher probability of a major break down, causing a long-time break in the production. Production sites located in high cost industrial countries have the urgent need to keep their production costs as low as possible and their technologies progressive to maintain their entitlement for their existence.

2. Literature overview

2.1.Steel

2.1.1. Stainless steel

As an outcome of German and Britain engineering work, stainless steels were implemented the first time at the beginning of the twentieth century. Because of the useful characteristics of stainless steels plenty different kinds were developed for usage in the chemical, food, energy and other industries. Over the century the family of stainless steels increased its number of members and in the late 1920s the “standard grades were processed further and high-alloyed ”High Performance Austenitic Stainless Steels” HPASS grades were developed [1]. In order to obtain very low carbon and exact alloy contents, new steel-making technologies like argon-oxygen decarburization (AOD) and vacuum-oxygen decarburization (VOD) had to be developed and implemented. With better and better processes, a cost-effective performance of stainless steels could be ensured in the last century.

The commonalities of all stainless steels are an iron-based alloy with a minimum amount of chromium of 10.5%. Chromium reacts with oxygen in the air and builds up a passive layer which protects the subjacent material from further corrosion. Other alloying elements, depending on the desired properties, are for example Nickel, Molybdenum, Carbon, Nitrogen, Manganese, Copper, Silicon, Niobium, Columbium, Titanium, Sulfur or Phosphorus [2].

The family of stainless steels can be subdivided in four different major categories regarding their microstructure: ferritic, austenitic, duplex (mixture of ferrite and austenite), and martensitic. The desired microstructure can be adjusted by the amount of alloying elements [3].

2.1.2. Influence of alloy elements

To improve the properties of stainless steels, different elements are added to the iron-based melt. On the one hand there are intentional elements, which are added to influence for example the metallurgical structure, mechanical properties, physical properties or corrosion resistance, and on the other hand the steel contains unintentional alloying elements, which could not be removed completely [1].

There are two different possibilities for alloying elements to be incorporated in the crystal lattice. Elements like chromium, nickel and molybdenum find their place on the substitutional sites of the lattice [4]. A necessary precondition for this configuration is nearly the same size of the atoms, with a possible deviation of 15 %, the same lattice configuration of crystal "A" and "B" and chemical affinity of the components [5].

Other elements, like carbon and nitrogen, are positioned in the open spaces between the lattice atoms, which are called interstitial sites [6] [7]. This results in the creation of long-ranged strains within the lattice, which turns them to potential hardening elements [1]. The precondition for this arrangement is the much smaller size of these interstitial atoms compared to the lattice atoms.

The type and content of the different alloying elements have a strong pronounced influence on the properties of the material. It is necessary to be taken in consideration which property is more important for an application, in order to obtain the desired characteristics of the material. Some elements are beneficial, some are detrimental for a specific property. In the following section, the most important influence of different alloying elements is described.

Carbon:

Carbon, as mentioned before, is an interstitial alloying element, which is a potent hardening element. In order to keep the weldability and the corrosion resistance high, the carbon content is held in the hundredth percent range. Because of the high affinity of chromium to carbon, chromium carbides precipitate on the grain boundaries and form a chromium depleted zone around them. This is a weak point for intergranular corrosion. (Fig. 2-1) [8].

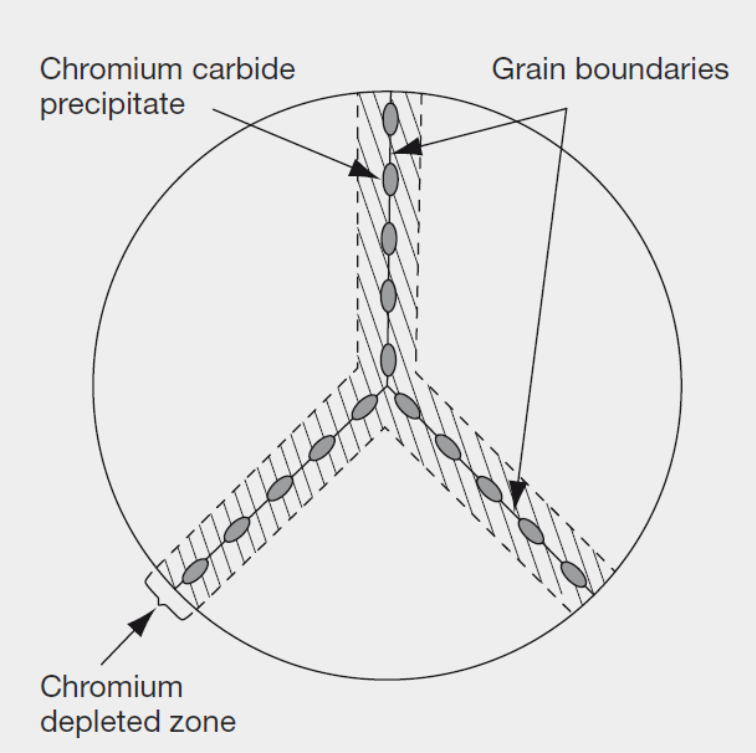

Fig. 2-1: Schematic representation of sensitized grain boundaries in an austenitic stainless steel [8].

Therefore, the carbon content of most austenitic steels is limited to the lowest practical levels. One the positive site, carbon strengthens the austenite, which is useful for boiler tubes, which operate at high working temperatures [1]. Another way to stabilize the austenitic phase is to add Niobe or Titanium [9].

Chromium:

A chromium content of at least 10.5 % is essential for stainless steels [10]. Chromium is responsible for the protective passive layer, which shields the stainless steel from environmental influences, which includes aggressive waters, many acids and even highly oxidizing high-temperature gases. In combination with Aluminum and Silicon [11] it also protects stainless steel from high temperature corrosion. In Duplex steel, higher chromium contents stabilizes the ferrite phase, nevertheless nickel has to be added in order to obtain an austenitic or ferritic-austenitic microstructure [1].

In combination with carbon, chromium tends to build carbides (Fig. 2-1), depending on the temperature and the time of the heat-treatment process. Fig. 2-2 displays the influence of

time and temperature at the cooling process in a Time-Temperature-Transformation diagram (TTT) of a 316 stainless steel.

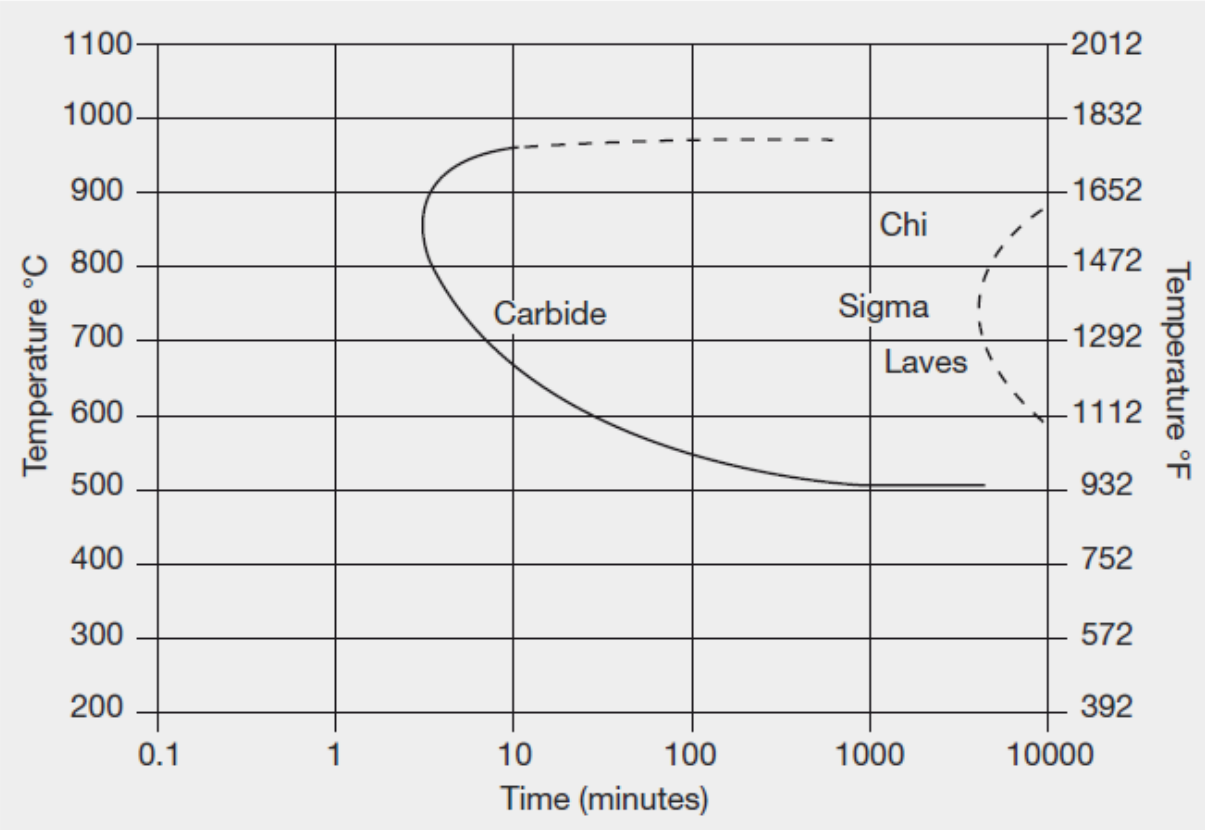

Fig. 2-2: TTT diagram of a 316 stainless steel. Secondary phases like Chi, Sigma and Laves need more than 1000 minutes to develop in this standard grade stainless steel [12].

Nickel:

The main purpose of Nickel is the stabilization of the austenitic phase. Nickel improves the mechanical properties of stainless steels to a certain amount. Adding nickel also delays the formation of undesirable intermetallic phase in austenitic steels.

Nickel also improves the corrosion behavior in certain reducing acids and it also increases stress corrosion resistance with alloy contents of about 20 %. Moreover, Nickel has the ability to decrease the rate of work hardening during cold deformation [1].

Molybdenum:

Because of the fact that Molybdenum forms undesired intermetallic phases, its content is limited to 2 % for standard austenitic grades, such as 316L, and up to 7.5 % for HPASS steels

[10]. In combination with chromium it increases the resistance against pitting. Above a chromium content of 18 %, Molybdenum additives develop a up to three times better resistance against pitting and crevice corrosion [13, 14].
The disadvantage of molybdenum is its property to stabilize ferrite and to build undesirable intermetallic phases.

Nitrogen:

Nitrogen is a cost-effective alloying-element. One of its properties is the stabilization of austenite and is therefore used to replace Nickel to a certain amount. It also retards carbide sensitization, the formation of secondary phases and the formation of sigma phases in high chromium- and molybdenum-alloyed steels. In low carbon alloys, small amounts of Nitrogen (about 0.1 %) [1] are also used to counteract the loss of strength of the material whereas in standard grades and HPASS it is used to rise the strength [15] by increasing the stacking fault energy.
Another ability of nitrogen is the reduction of the susceptibility for chloride pitting and crevice corrosion. Therefore, some of the high performance HPASS can contain up to 0.5 % Ni [1].

Manganese:

In order to deoxidize molten steels, manganese is used in steel metallurgy. Therefore, a small amount of this alloying element is used in all stainless steels.
Another important property of Manganese is the stabilization of austenite to room temperature [16]. It also increases the Nitrogen solubility, so it is added to HPASS to allow higher nitrogen contents which improve the strength and corrosion resistance as mentioned before.

Silicon:

Similarly, to Manganese Silicon is used to deoxidize molten steel, so small amounts are always used in stainless steels. In cooperation with manganese and other deoxidizing elements, present as small oxide inclusion, it has effects on the surface quality, polish ability, weldability and also corrosion resistance [17].

Sulfur and Phosphorus:

The phosphor content in alloys is always kept as low as possible because of the fact, that it has detrimental effects on the material. An unfavorable effect of Phosphorus is deterioration of the hot workability during forging and hot rolling [18].

Sulfur has similar detrimental effects like Phosphorus. Its most favorable effect is the increase of machinability. Nevertheless, the sulfur-content is kept very low, to about 0.001 % [1].

2.1.3. Microstructure

Elements like Iron, Chromium, Molybdenum and Silicon belong to the ferrite formers, whereas Nickel, Nitrogen, Carbon and Manganese are considered as austenite formers [19]. In order to get a rough overview on the influence of chemical compositions on the amount of ferrite and austenite in the microstructure of as-cast weld metal the Schaeffler Diagram can be used.

The Schaeffler Diagram (Fig. 2-3) allows to obtain information of the microstructure of the stainless steels depending on their chemical composition using the chromium and nickel equivalent.

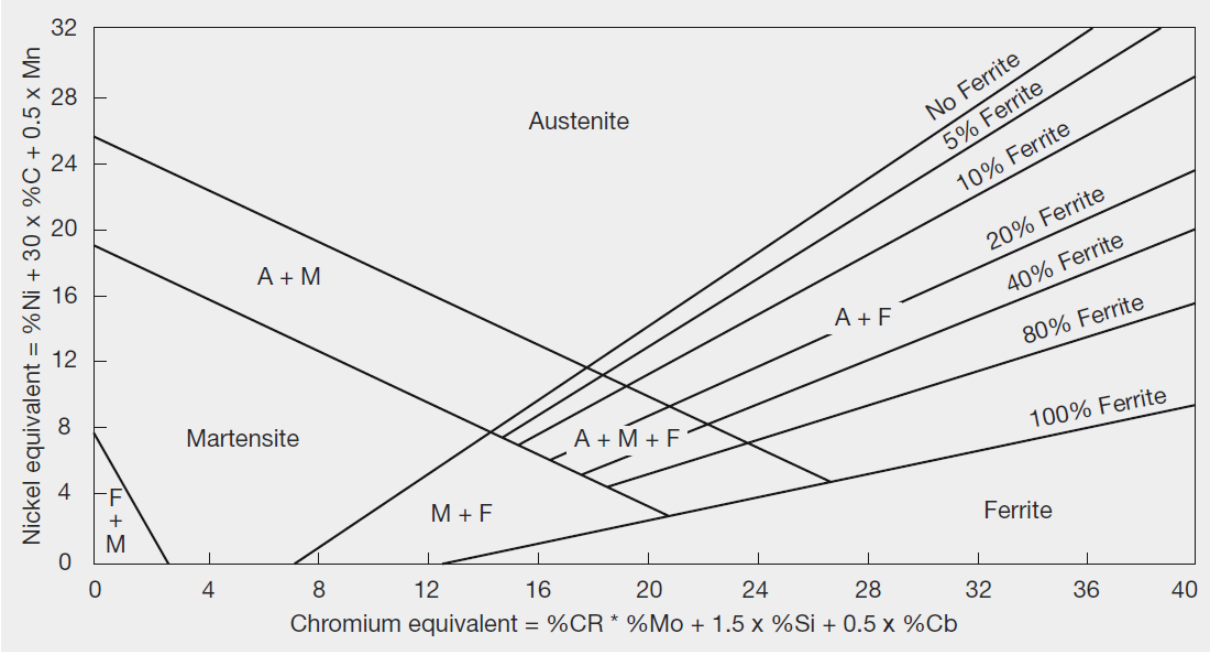

Fig. 2-3:The Schaeffler Diagram showing the different microstructures depending on the content of the alloy elements [20].

Formula 2.1, which is referred to as chromium equivalent, defines the value listed on the abscissa of the diagram:

$$chromium\ equivalent = \%Cr + \%Mo + 1.5 \cdot \%Si + 0.5 \cdot \%Cb + 2 \cdot \%Ti \qquad (2.1)$$

To obtain the value for the ordinate, the so-called nickel equivalent has to be calculated. Therefore, formula 2.2 is used:

$$nickel\ equivalent = \%Ni + 30 \cdot \%C + 0.5 \cdot \%Mn \quad (2.2)$$

Due to the fact, that in most cases other secondary phases can be formed after exposition to higher temperatures, also TTT diagrams should be taken in consideration to evaluate the mechanical properties of the material. Next to carbides and nitrides of chromium, also two other phases are formed. These are called sigma and chi phase and contain a high content of chromium and molybdenum. Because of the fact, that they are more like a chemical compound than a metal they are called intermetallic phases. Depleting the surrounding areas of chromium and molybdenum the corrosion resistance is lowered and the brittleness of the material is increased [21].

2.2.Cold forming

Cold-forming is the process of forging and forming metals at temperatures near to room temperature. Its purpose is to form metals with high speed and high pressure into various forms used for different applications. Beneficial side effects are the increase of yield, tensile strength and hardness via work hardening. Further advantages of cold forming compared to high temperature forming, are the dimensional accuracy after forming, the high surface quality and near optimum utilization of materials. On the other side, it has detrimental effects on the weldability of the material due to the substantial strain hardening leading to significant strength enhancement, which can be only solved with subsequently soft annealing [22].

Beside the cold-forming process there is also the possibility to form at higher temperatures, for example warm- and hot-forming. For steel, hot forming works in a temperature rate which leads to austenitisation. This range starts at about 60 percent of the melting temperature which is for ferritic steels around 850 °C. Whereas, warm-forming processes work in a temperature range of 600 °C to 900 °C for stainless steels. One of the main advantages of warm- and hot-forming is the lower force needed to form the material. On the downside, a scaly surface and dimension inaccuracies appear with these processes. One important point is the microstructure of the final material. With higher temperatures changes in the microstructure and formation of carbides or other brittle phases are more likely due to the higher diffusion rate.

Cold forming is established for many years in the industry and therefore a well-controlled process. Nevertheless, great effort is put into research and development of new methods, improvements and further scopes of applications.

An upcoming new generation of cold formers work with servo-motors in order to increase the possibilities of using different and more complex cold forming processes. It combines the accuracy and reliability of the well-known mechanical processes with the flexibility of a hydraulic process which allows infinite variable slide speeds and position control [23]. With different speeds within the cold forming process based on exact positions it is possible to avoid typical failures such as underfilling or overfilling and it allows to cold form more complex geometries and higher-strength steels.

In order to make further improvements in the field of cold forming, as well as other fields of production and manufacturing, digitalization and extensive monitoring has gotten more important in the past years. All these improvements can by summarized in the term industry 4.0. The main idea of industry 4.0 is to digitalize and link manufacturing processes in order to spare costs and to increase the quality and the productivity [24]. Huge potential is seen in monitoring and in in-situ controlling of tools and material in order to avoid crashes and fast tool wear. One way to achieve this, is the concept of predictive maintenance, where sensors are monitoring different parameters of the forming process, as forces and vibrations, combined with a software which evaluates them, pursuing the target to predict tool wear and crashes. Therefore, tools which are close to a critical wear can be changed upfront and a crash with further tremendous consequences can be avoided. [25]. Another approach is to monitor the health of the tool itself. In doing so the tool breakage can be avoided which extends the health and endurance of the cold former. This process is more common at milling machines but there is also great potential for cold formers [26].

Another approach to reduce costs at the cold forming process leads to research work in the field of tribology. The idea is to cold form without lubricants like oil or emulsion. To achieve this, different coatings and lubricants within the tools are tested. [27, 28]. The implantation of dry forming is desirable for both economic and ecological reasons. The main focus is on the prevention of adhesion effects of the tools.

Looking at the tool geometry and tool costs one possible next step will be additive manufacturing. Using this method, it is possible to realize complex geometries and various functionalities of tools. It would be imaginable to add a sophisticated cooling system within rolling dies or high complex geometries in forming dies. Due to the precise manufacturing subsequent machining process will be faster and cheaper. For now, additive manufacturing processes are neither as fast and accurate as traditional metal forming processes as milling, casting and forming, nor is it possible to receive the desired surface quality [29]. Another big issue is the lack of density of materials produced by additive manufacturing compared to traditional manufacturing methods which has a big influence on the mechanical properties like hardness, stiffness and strength [30].

Another future technology being researched is the concept of massive lightweight design. By using an intelligent multi-component process, it is possible to approach a still tough lightweight design. To achieve this, different materials are used in one component by cold

forming. By using various materials for different parts of the component it is possible to adapt the properties as good as possible to the later application of the component. Therefore, it is possible to realize a lightweight, high-strength and multifunctional final product with high durability. For example I the field of gear wheels lot of potential is seen [31].

2.3. Forming behaviour

Each material has a slightly different behavior regarding its abilities for cold forming. Some of them are more suitable like unalloyed low carbon steels, others less like thermo-mechanical treated steels. The deformability dependents on the chemical composition of the material, the microstructure, the forming speed and the temperature.

Stainless steels are used for cold forming processes ranging from simple bending to complex deep drawing. Cold formed, they show a unique assembly of advantages, for instance high to ultra-high strength next to high ductility. Cold-forming operations which lead to complex component geometries of austenitic stainless steels in some cases replaces metalworking and welding operations traditionally used to obtain the wanted component geometry and increases the corrosion resistance [32].

In order to obtain the ability to cold form, the content of Silicon may not exceed 3 %, the content of Boron must not be more than 0.002 % and the content of Nitrogen should not exceed 0.1 %. To decrease the work hardening rate while cold forming, Nickel plays a crucial role [1].

Austenitic stainless steels cannot be hardened by heat treatment. Therefore, the process of cold forming itself is used to harden these steels, accountable therefore is the effect of work hardening. Work hardening, or strain hardening, is the effect most metals show during forming processes. They become stronger and harder, the higher their plastically deformation is. Therefore, higher deformations require higher forces [33]. By increasing the temperatures, the rate of strain hardening is lowered [34]. Responsible for the phenomenon of work hardening are the dislocations in the material occurring during forming processes. The higher the force on the material, the more dislocations occur which leads to plastic deformation [19]. Because of this, the tensile strength of the material is increased, as can be seen in Fig. 2-4 for various stainless steel grades.

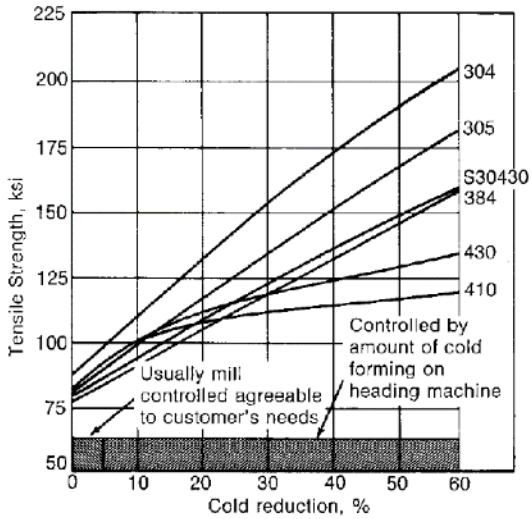

Fig. 2-4: The increase of the tensile strength with higher degrees of deformation of stainless steel for cold forming [35].

Besides the reduction grade also the forming speed $\dot{\varphi}$ influences the yield strength and the forming behavior of the final material. With increasing deformation speed, the yield strength increases as can be seen in Fig. 2-5 for the grade 100Cr6, which is a martensitic chromium rolling bearing steel.

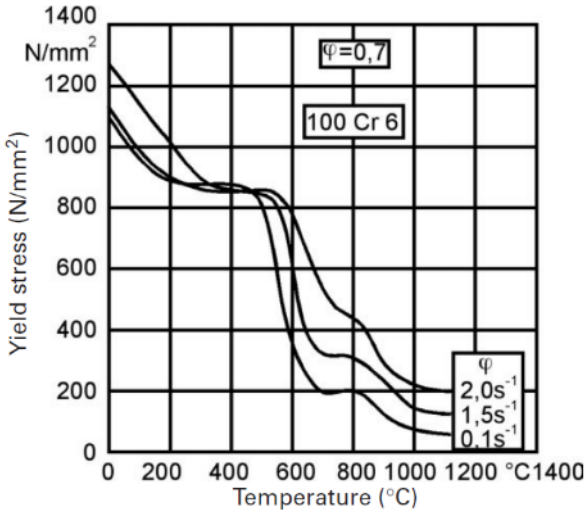

Fig. 2-5: The dependence of the yield strength on the temperature for different forming speeds [36].

Considering Fig. 2-5 the flow stress around 700 °C is higher for faster forming speeds by nearly a factor of 2-3. This can be described by the effect of recrystallization which has more impact on the microstructure and therefore on the yield strength at lower forming speeds

than it has at higher. This is because of the fact, that recrystallization is a diffusion-controlled process, which is depending on temperature and time [36].

Austenitic stainless steels show the effect of a spring-back effect at the process of bending which means, that the elastic amount of the deformation forms back. Steels with higher nitrogen content and steels rolled to increase yield strength are more vulnerable for spring-back than standard grades. Fig. 2-6 shows a high strength duplex stainless steels, comparable to austenitic steels with high nitrogen contents or with increased yield strength, in comparison with a standard grade 316 austenitic steel.

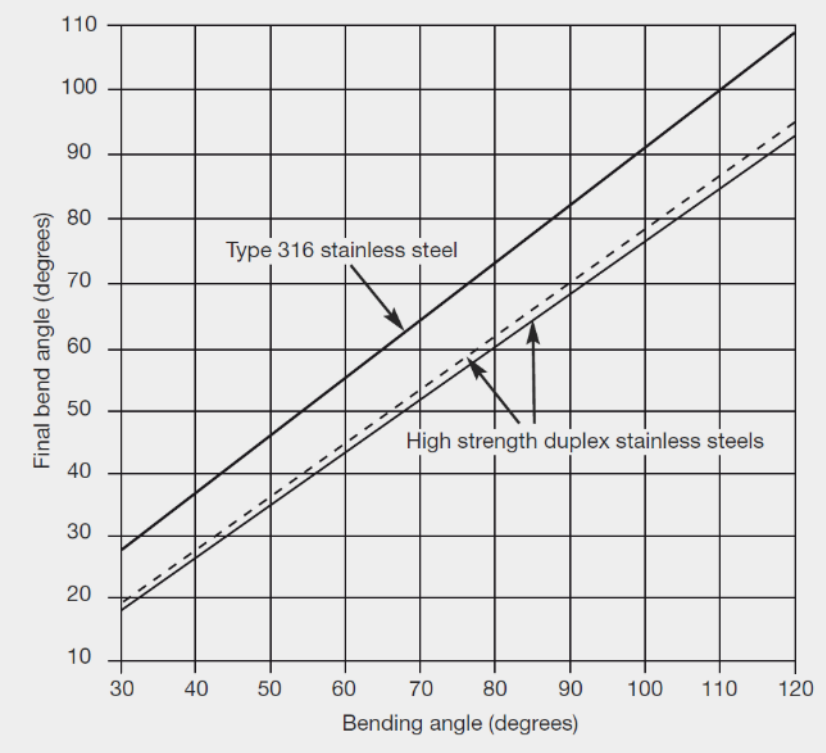

Fig. 2-6: Visualization of the spring-back effect for standard and high strength duplex stainless steels [37].

Another major impact on the forming behavior has the coating of the wire in the case of cold drawing and therefore extrusion. The coating in combination with the lubrication defines the friction coefficient between the wire and the forming die which has a big influence on the flow properties of the material [38].

In contrast to unalloyed and low-alloyed steels it is not possible to use a general zinc-phosphate coating for stainless steels [39]. The most common system used as replacement is

the iron-oxalate coating which is applied similar to the zinc-phosphate coating with pickling and film formation [40].

For smaller degrees of deformations and lower forming forces, as it is most common for the thread rolling production of screws, another alternative to the zinc-phosphate coating is a salt-lubricant-carrier layer. In combination with oil it ensures a coating for the forming process. At higher temperatures and pressures molybdenum disulphide is added to the salt-lubricant carrier layer or used by itself [41].

For environmental protection single-layer lubricant systems on the basis of polymers or salt-waxes are getting into focus. The major advantage is the prevention of chemical bathes as well as their resulting waste products. For this case it is possible to use similar systems as used for unalloyed or low-alloyed steels [42].

2.4.Yield strength

Generally, yield strength is the term for stress, at which plastic deformation occurs in a material for the first time, as shown in Fig. 2-7. There are several terms defined for this point, but the term, yield strength, is the most common.

For technical materials, usually the offset yield strength or proof stress ($Rp_{0,2}$) is used. It is the stress at which 0.2 % of plastic deformation occurs and remains after releasing the load. In Fig. 2-7 the Yield strength is marked with the number 1, whereas the offset yield strength is tagged with number 2.

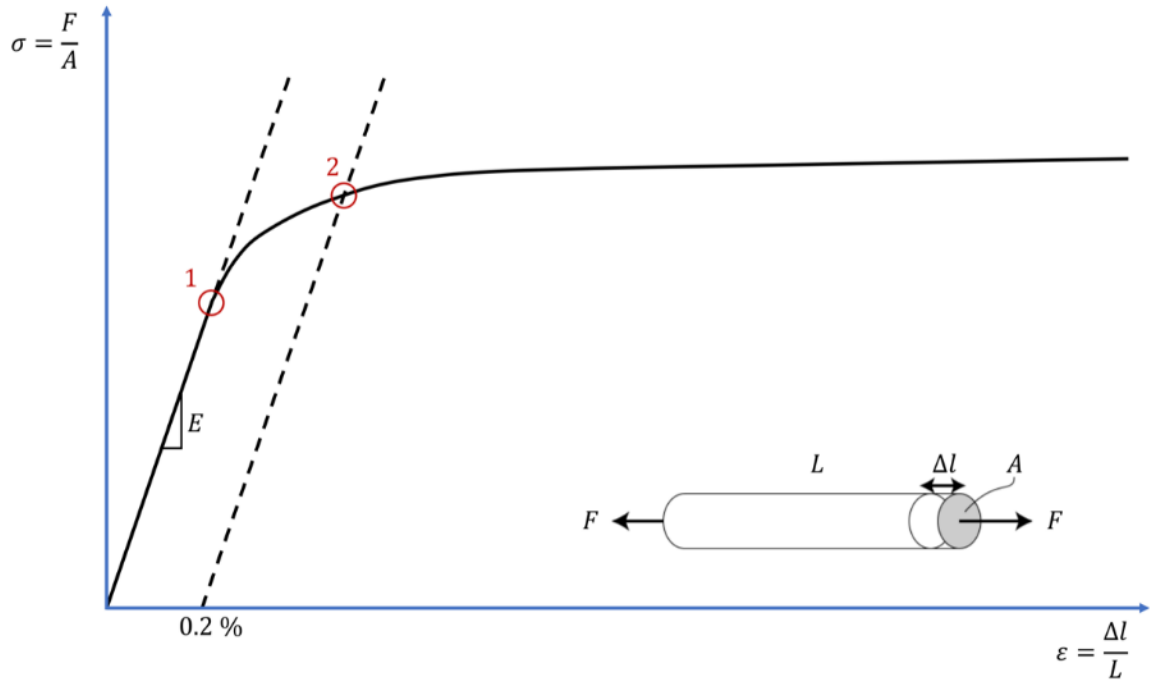

Fig. 2-7: Stress-strain-diagram showing the yield strength (1) and the offset yield strength (2).

Crucial for most engineering designs, the yield strength is mainly influenced by raw material quality, chemical composition, forming process, heat treatment and various other factors. It is commonly measured using a load versus displacement method, for example according to ISO 6892-1:2016, at room temperature and 1 atm [43].

The typical stress-strain curve for austenitic stainless steels lies between the curve of ferritic and duplex stainless grades, as shown in Fig. 2-8. The yield strength of austenitic steels is in

the range of 200 MPa for very soft materials up to 2000 MPa for materials after cold working [44].

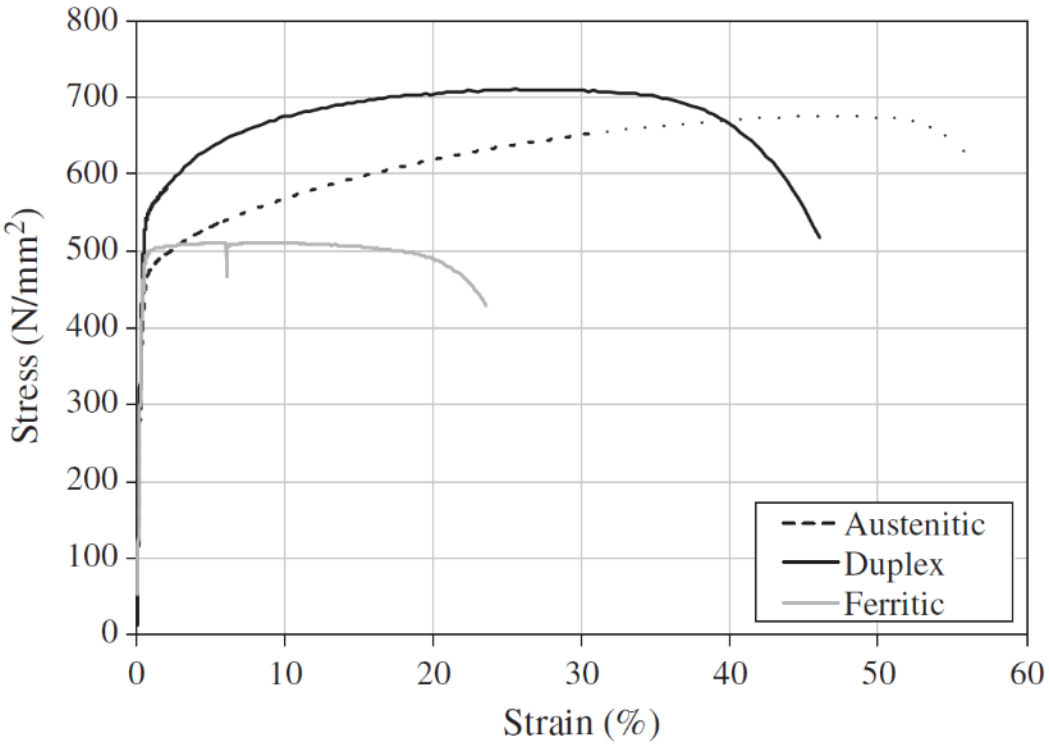

Fig. 2-8: Typical stress-strain curves for austenitic, ferritic and duplex stainless steel grades [45].

The yield strength of a material can be increased by strain hardening or cold working. This is especially used for materials, which do not harden at the process of heat treatment like stainless steels. Cubic metals have a higher strain hardening rate, than hcp metals. In general, the rate of strain hardening corresponds to the slope of the flow curve. By increasing the temperatures, the rate of strain hardening is lowered. In Fig. 2-9 the typical variation of strength and ductility parameters with increasing amount of cold work can be seen. Because of the fact, that cold forming processes are commonly one or two dimensional, it results in an elongation of the grains [34].

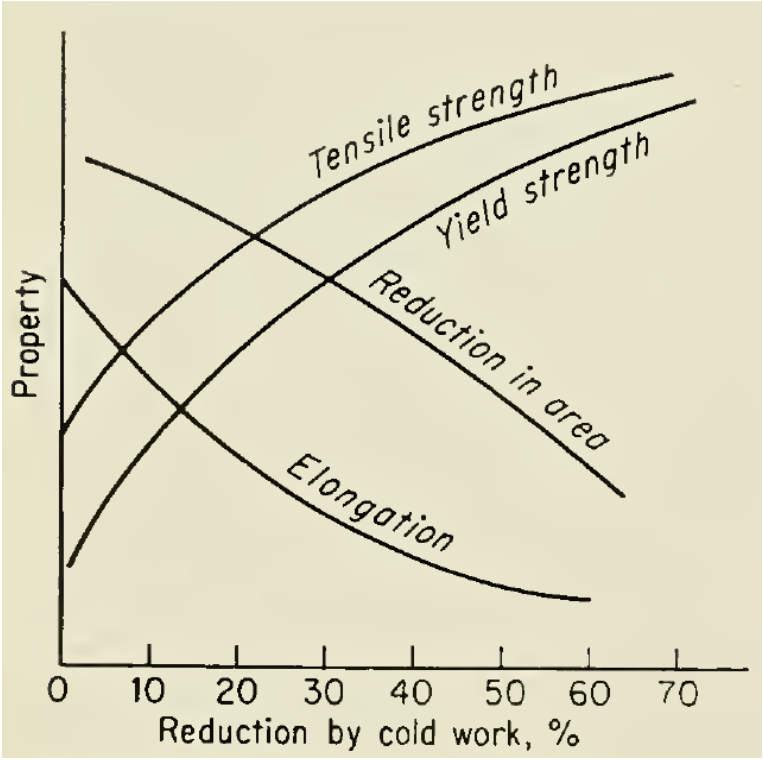

Fig. 2-9: Dependence of the tensile strength, the yield strength, the reduction in area and the elongation on the reduction by cold work [34].

3. Experimental

3.1. Material

For the experimental part of this thesis the material 1.4404 was used. It is an austenitic stainless steel of the grade Type AISI 316L. Other terms for this material are A4, V4A, SS316 or X2CrNiMo17-12-2. 1.4404 is mainly used for mechanical components with high requirements on corrosion resistance, especially in chloride containing mediums and hydrogen. Other utilizations are in the pharmaceutical, medicine, dental, automotive and aircraft industry as well as mechanical engineering and for the construction of swimming pools [13].
The range of the chemical composition of this material is listed in Table 3.1.

Table 3.1: Chemical composition of grade Type AISI 316L [46].

	C	Si	Mn	P	S	Cr	Ni	Mo	N	Cu
min	-	-	-	-	-	16.5	10.0	2.0	-	-
max	0.03	1.0	2.0	0.045	0.03	18.5	13.0	2.5	0.11	1.0

In order to describe the microstructure of the material the Schaeffler diagram is used, as described in 2.1.3. Formula 3.1, which is referred to as chromium equivalent, defines the value listed on the abscissa of the diagram:

$$chromium\ equivalent = \%Cr + \%Mo + 1.5 \cdot \%Si + 0.5 \cdot \%Cb + 2 \cdot \%Ti \quad (3.1)$$

Calculating with the typical average composition of the material a chromium equivalent of 19.23 is obtained, shown in 3.2.

$$16.74 + 2.01 + 1.5 \cdot 0.32 + 0.5 \cdot 0 + 2 \cdot 0 = 19.23 \quad (3.2)$$

To obtain the value for the ordinate the so-called nickel equivalent must be calculated. Therefore, formula 3.3 is used:

$$nickel\ equivalent = \%Ni + 30 \cdot \%C + 0.5 \cdot \%Mn \tag{3.3}$$

With the typical composition of the delivered raw material a nickel equivalent of 12.24 is received.

$$11.03 + 30 \cdot 0.015 + 0.5 \cdot 1.51 = 12.243 \tag{3.4}$$

Using the Schaeffler Diagram the amount of ferrite and austenite can be determined roughly. As seen in Fig. 3-1, the content of ferrite in the microstructure should be around 5 % and the content of austenite about 95 %.

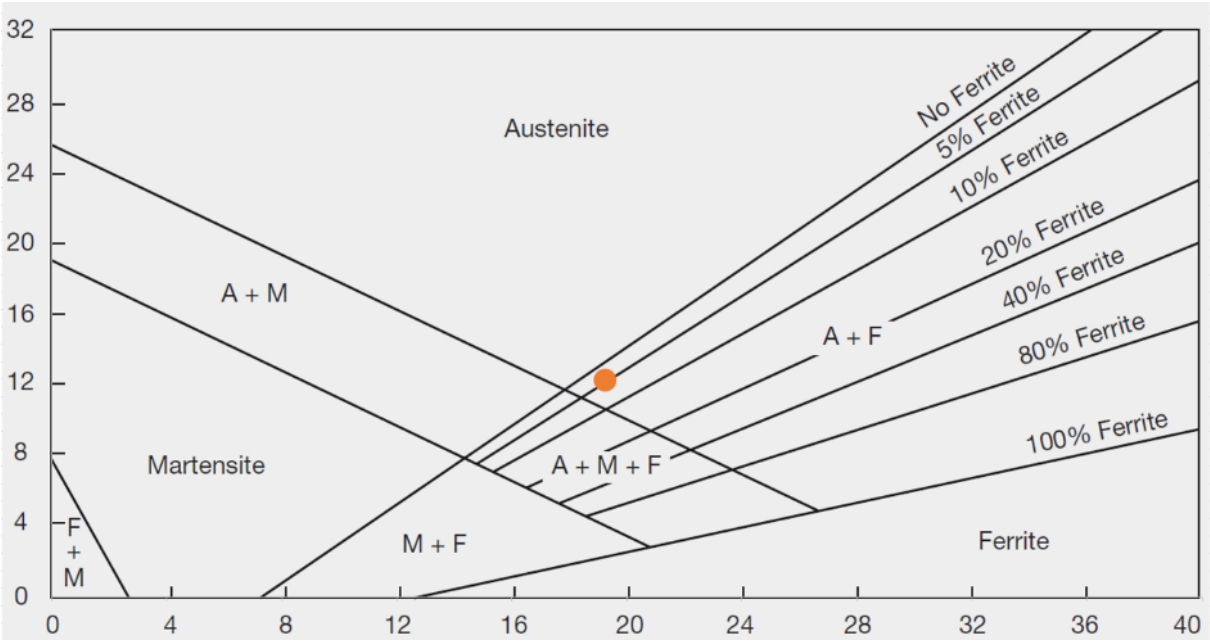

Fig. 3-1: The Schaeffler Diagramm roughly shows the microstructure of the used stainless steel [20].

Fig. 3-2 shows the Time-Temperature-Transformation diagram of the standard grade AISI 316 which has nearly the same chemical composition as the AISI 316L besides a maximum carbon content of 0.07 % instead of 0.03 %. The tests, which are executed within the scope of this thesis, range all in a temperature field from room temperature to 150 °C. In this area, no formation of secondary phases and carbides is expected.

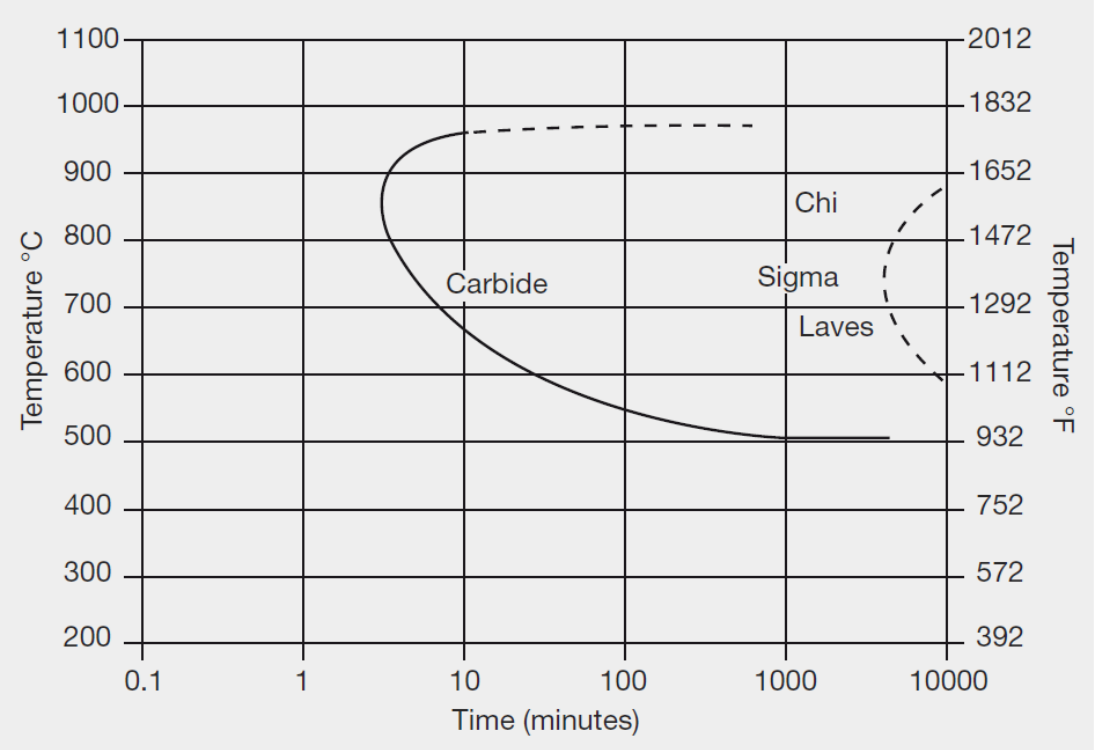

Fig. 3-2: Time-Temperature-Transformation diagram for AISI 316 standard grade stainless steel [47].

3.2. Used product

The product, which was investigated within the experimental part of this thesis, is the Hilti HUS-HR 10, which is an ultimate performance screw anchor with a hexagonal head (Fig. 3-3). The HUS-HR 10 is available in 7 different lengths varying from 65mm in decimal steps to 115mm and the longest is 130mm.

Fig. 3-3: Picture of the Hilti HUS-HR 10x95.

The stainless steel screw anchor is manufactured out of stainless steel 316L and is used for cracked und uncracked normal-weight or lightweight concrete. The anchor is capable to be used for seismic applications [48].

Due to the short tool lifetime and the high degree of deformation this product was choosen for the preheating tests. Another reason is the high degree of deformation the wire is exposed.

The raw bolt is formed in a 5-step process (Fig. 3-4). Within the process, the wire is formed through increasing and decreasing of the diameter into a raw bolt. In the next step the thread is rolled on the bolt, which finalizes the geometry of the product. Finally, hard metal barrels are welted on the thread to improve the performance of the screw during application.

Fig. 3-4: Geometry of the HUS-HR 10x65 after each forming step and after thread rolling.

The most important dimensions for the final function of the product, according to the application performance and load class of the screw bolt, are the length of the screw, the inner and outer diameter of the thread and the length of the thread. These are the main parameters which were controlled after the tests.

3.3. Experimental setup

3.3.1. Crush test

To evaluate the influence of different temperatures on the yield strength and the flow properties of the used material, crush tests were performed. At first instance, tests were done on a UPM Zwick & Roell "Zwick 1485" (Fig. 3-5) in the department TM Materials and Manufacturing at Hilti AG. One of the main goal of these tests was to find a production near method to get a rough idea of the influence of temperature on materials in order to improve the results of computer-aided numerical simulations and to plan further tests in the production. To evaluate the results an additional crush test on a Servotest TMTS was performed at to the "Chair of Metal Forming" at the "Montanuniversität Leoben" (hereinafter referred to as CMF).

Fig. 3-5: UPM Zwick & Roell "Zwick 1485" used for the crush tests at Hilti AG.

The crush tests at the UPM Zwick & Roell "Zwick 1485" were performed at 6 different temperatures: room temperature, 200° C, 250° C, 300° C, 350° C and 400°C. Due to the functionality of the chamber furnace, lower temperatures were not possible. The environmental conditions for all tests were held constant with an air pressure of 1 atm, a testing speed of 2 mm/s and a preload of 2 MPa. In order to minimize the friction between the samples and the test device, oil was used. For performing the tests, sample with a length of 17.25 mm and a diameter of 11.5 mm (see Fig. 3-6) were produced in order to achieve a length/diameter ratio of 1.5 which is in the range (formula 3.5) recommended in DIN 50106:1978-12 [49] using the given diameter of the wire. The length as well as the diameter were determined before and after the test.

$$1 \leq \frac{h_0}{d_0} \leq 2 \tag{3.5}$$

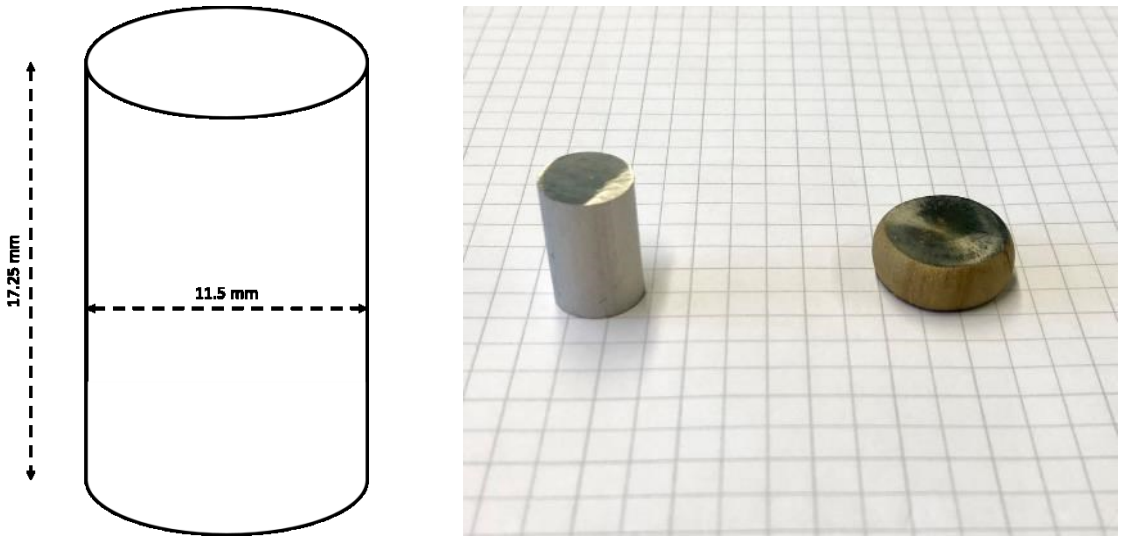

(a) (b)

Fig. 3-6:(a): Schematic drawing of the sample geometry, (b): picture of the sample before the test and after the test at 400° C.

To warm up the samples to the desired temperature, a chamber furnace (Fig. 3-7) was used. At each temperature 3 samples were tested. Starting at 200 °C the temperature was increased by 50° C after each set of tests, up to 400° C. The temperature was measured with a thermocouple which was positioned within a hole of one sample and connected to a

measuring computer. Therefore, the temperature of the sample core could be monitored in real time and the samples could be tested exactly at the desired temperature.

Fig. 3-7: Chamber furnace used to heat the samples for crush tests.

When the core of the sample reached a certain testing temperature, the sample was transferred quickly into the UPM Zwick & Roell “Zwick 1485” and the crush test was performed. Within the crush test at Hilti AG, overall 18 samples have been tested, 3 samples at 6 different temperatures.

To compare and evaluate the results, as mentioned before, a second series of tests has been performed at the CMF. To get a broader range of results 11 different temperatures, RT, 50° C, 100° C, 150° C, 200° C, 250° C, 300° C, 350° C, 400° C, 450° C and 500 °C, were tested. For each temperature 2 samples were used. The testing speed was 1 mm/s. The environmental conditions were chosen equally to the ones at the UPM Zwick & Roell “Zwick 1485”.

Like the samples used for the tests at the UPM Zwick & Roell “Zwick 1485”, the CMF used a length diameter ratio of about 1.5, which leads to a length of 18.6 mm and a diameter of 12

mm. Other than the simply samples, used at Hilti AG, the used Rastegaevsamples have a lubrication pocket on each side and a hole for the thermocouple (Fig. 3-8).

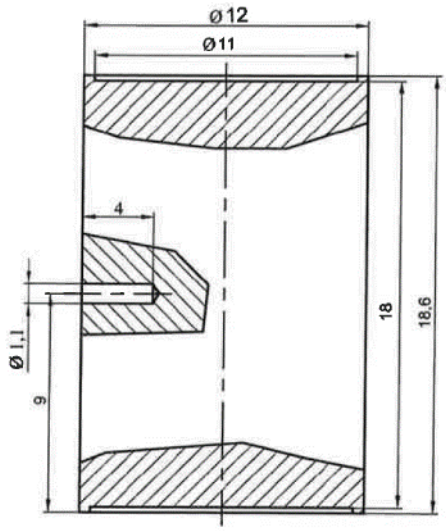

(a)

(b)

Fig. 3-8: (a): Schematic drawing of the Rastegaevsample [50] geometry (all dimensions in mm), (b): picture of the sample before the test and after the test at 400° C.

3.3.2. Preheating

The process of preheating and the associated tests were processed on a 235 ton 5-die metal cold former in plant 1 at Hilti AG in Schaan. The cold former from the company “NEDSCHROEF Machinery” is also used for the standard serial production of the HUS-HR 10 amongst various other stud- and screw anchors. The product HUS-HR 10 was used for all tests for preheating of the wire prior to the cold forming process.

In order to heat the wire an electrical inductor was used. The inductor was powered by a medium-frequency converter out of the MU series form the company “Himmelwerk Hoch- und Mittelfrequenzanlagen GmbH”. The MU consists of a converter and an external unit which powers and cools the inductor. The used MU-25 (Fig. 3-9) is the smallest model of the MU series and provides a power of 25000 Watt. The range of its frequency, dependent on the heated material, extends from 8000 up to 50000 Hertz. The converter provides three different working modes which are “push-to-run”, “time-dependent-run” and an external mode controllable through a port [27].

To supply water for the cooling system a 1000 litre intermediate bulk container (IBC) and a customary water pump was used to cool the converter and the inductor. The whole system is connected with water hoses and power cables.

Fig. 3-9: Generator of the Himmelwerk MU-Series.

For preliminary tests, in order to evaluate the functionality of the system and to estimate the heating- and cooling-time of the wire, the equipment was assembled and tested before the integration into the cold former was done. At the preliminary tests the used wire was positioned stationary in the inductor without the ability and intention to move. Therefore, the influence of the potential on the wire was only tested on the static system. For these simple tests the “push-to run” mode was used.

The actual tests took place at the 235 ton 5-die metal cold former. In order to synchronize the wire feeder with the inductor, the converter was controlled in external mode through a connection with the cold former. Too much heating of the wire could lead to an expansion of the diameter of the wire which would lead to a crash or in extreme cases may melt the wire. This is necessary to avoid, that the inductor heats up the wire when the wire feeder stands still. In this case the wire would reach too high temperatures and cause damages of the cold former. The inductor was positioned in the cold former as near as possible to the forming dies. Therefore, the inductor was positioned between the linear wire feed and the shear blades as can be seen in Fig. 3-10.

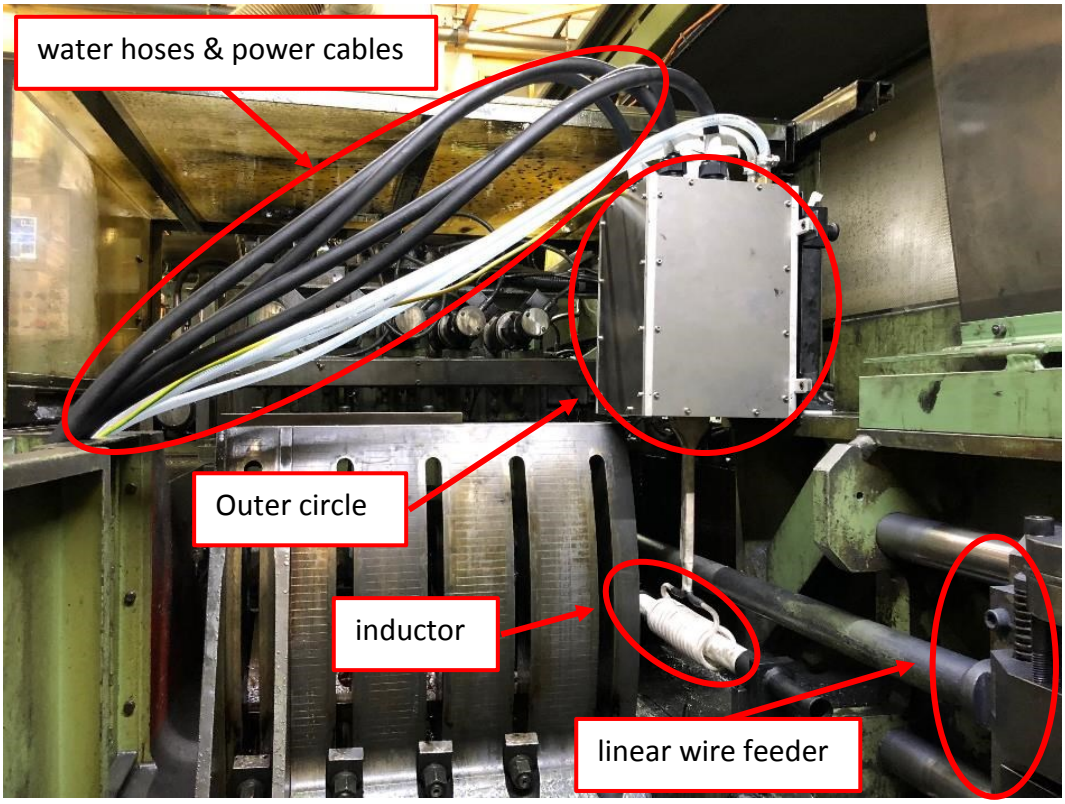

Fig. 3-10: The position of the inductor needs to be as near as possible at the dies to avoid too much cooling time of the wire.

In the standard production, a metal tube holds the wire in position and transports the oil used for greasing. This metal tube was replaced by a ceramic tube which is resistant to electrical coupling with the inductor and protects the inductor from damage by the wire. The converter and the intermediate bulk container were positioned outside of the cold former and the water hoses and power cables have been laid through a small opening in the cold former (Fig. 3-11).

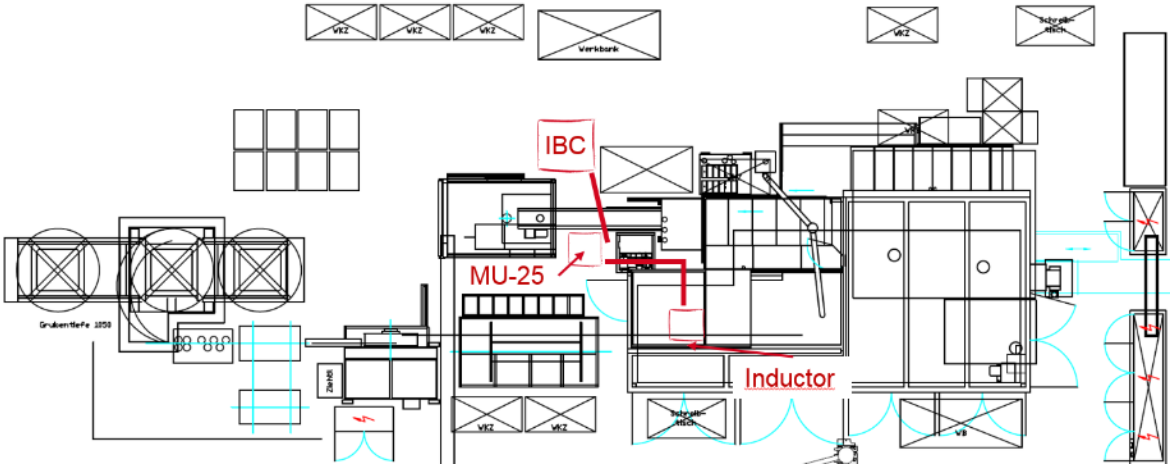

Fig. 3-11: Map of the cold former with the position of the inductor, converter and the cooling system.

On the way to the inductor the wire takes several other stages in the cold forming line. These stages are summarized to the umbrella term “wire line”. The wire line starts with the rotary blade, which unrolls the wire coil. To guaranty a constant diameter of the wire a draw blade is used in the next step and after this a barrel is used to pull the wire and move it forward. To achieve a straight form of the wire on the next step horizontal and vertical straightening rolls are used. The next and last step of the wire line is the linear wire feeder which subsequently leads to the inductor.

After the inductor there is approximately a two-meter long gap to the shear blades, which cut the wire into the right lengths for the forming process. Right after the shear blades the wire moves into the first die of the cold former which is followed by additional four dies. Each die forms a different step of the whole bolt. After the fifth die the half-done pin is moved to the last station in the forming process, which is the thread roller.

4. Results

4.1. Temperature-dependant yield curve

In order to define the influence of the temperature on the yield stress at different degree of deformation crush tests were performed. To evaluate the results two different test aggregates were used. On the one hand a UPM Zwick & Roell “Zwick 1485” and on the other hand a Servotest “Thermo-Mechanical Treatment Simulator” (hereinafter referred to as Servotest TMTS).

4.1.1. UPM Zwick & Roell “Zwick 1485”

The average values of the yield strength, enforced as described in 3.3.1, of three samples for each temperature were determined and plotted in a flow stress versus degree of deformation diagram as can be seen in Fig. 4-1.

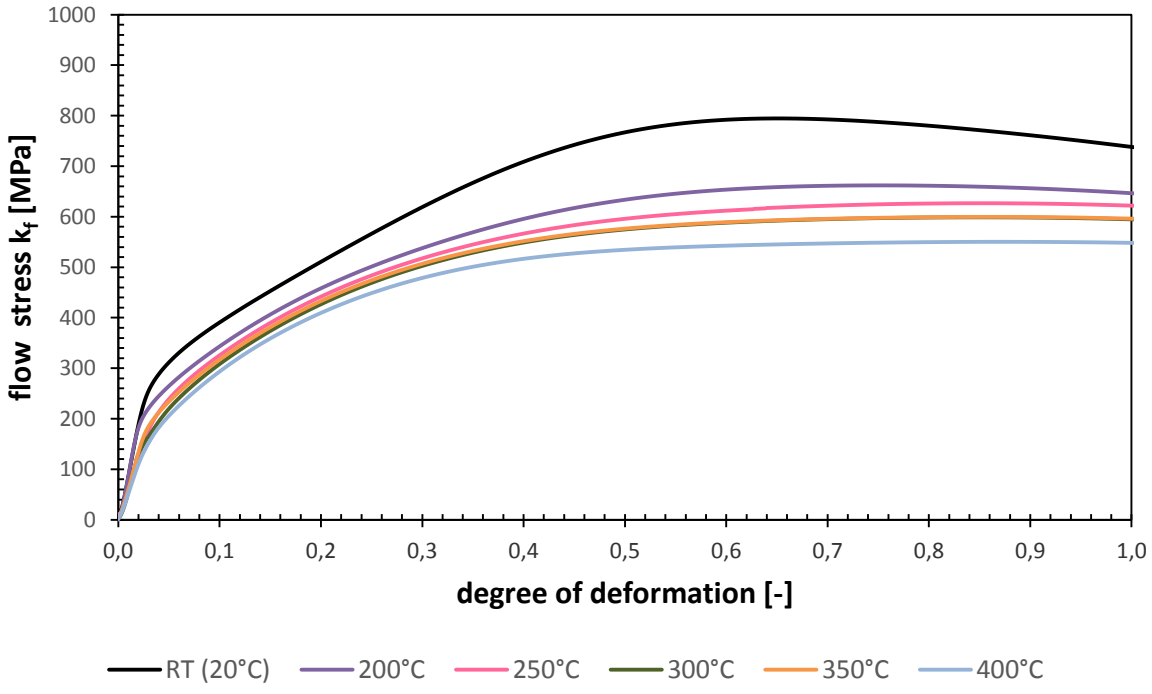

Fig. 4-1: Measured flow curves of 1.4404 at different at the UPM Zwick & Roell “Zwick 1485”.

The results of the crush test were as expected. With rising temperature, the force decreased. The results can be seen in Table 4.1.

Table 4.1: Temperature dependent results of the crush tests at UPM Zwick & Roell "Zwick 1485".

Testing temperature [° C]	Maximal yield strength [MPa]
20	795
200	662
250	627
300	599
350	600
400	550

4.1.2. Servotest TMTS

The results for the tests at the Servotest TMTS can be seen in Fig. 4-2. For each temperature the average value of the two samples is shown.

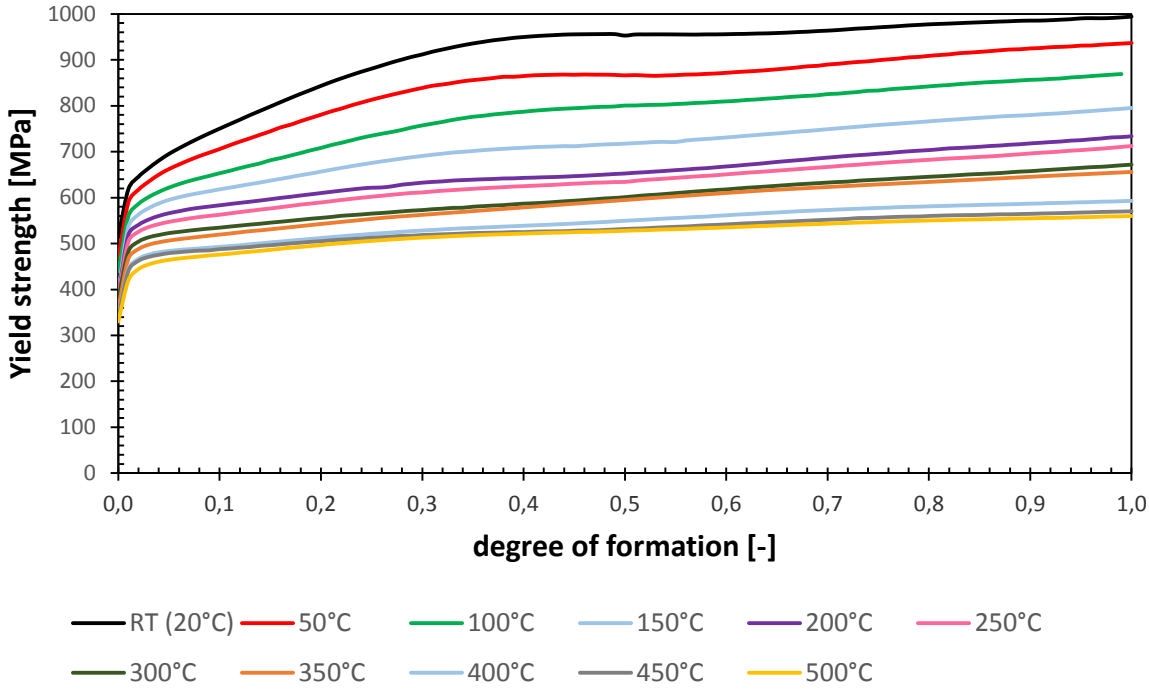

Fig. 4-2: Measured flow curves of 1.4404 at different temperatures at the Servotest TMTS.

Table 4.2: Temperature dependent results of the crush tests done at the Servotest TMTS.

Testing temperature [° C]	Maximal Yield strength [MPa]
20	994
50	937
100	871
150	795
200	734
250	712
300	672
350	656
400	593
450	570
500	560

As expected the forces drop with rising temperature.

4.2. Preheating

In order to setup the test a longer downtime of the used cold former was needed, as the inductor, the outer circle of the generator, the water hoses and power cables had to be installed in the cold former near the linear wire feeder. For the handling of the cold former during the experiment an experienced employee was needed. All in all, three attempts of preheating the wire during actual production conditions were done.

4.2.1. First attempt

The first wire heating test with the MU-25 failed at the very beginning. In contrast to the later successful tests, the first test the MU-25 was performed in “push-to-work” mode by an intern. For this reason, it was possible to also heat the wire at machine downtimes. With increasing temperature of the wire, the diameter of the wire expands, which leads to complications at the shear blades, as wire gets stucked and is not able to move further. The linear wire feed tries to push the wire further. The result is a crash which bursted the ceramic tube and warps the inductor (Fig. 4-3).

Fig. 4-3: The crash after the malfunction of the inductor control leading to a failure of the ceramic tube and the inductor.

4.2.2. Second attempt

As a result of the failed first test, the MU-25 was linked via an external port to the linear wire feeder of the NB 520 L02. This connection controls the MU-25 so it only heats the wire in the case of a running linear wire feeder, avoiding overheating of the wire at unpredictable downtimes. As further step, the draw blade, which brings the wire to the final diameter, has been exchanged with a draw blade for smaller diameters. Instead of a diameter of 9.58 mm a draw blade for a diameter of 9.33 mm was used, which leads to a safety tolerance of 0,25 mm avoiding a crash at a higher thermal expansion.

Because of these adaptations, the second test was a success. To compare the results of the preheating test with the standard production, the cold former was operated at room temperature at first. Afterwards the generator was run with different potentials in order to heat the wire starting from lower temperatures and rising them during the test. Each potential lead to a different resulting temperature as can be seen in Table 4.3.

Table 4.3: Temperatures caused by different potentials measured with a hand-held contact temperature-measuring device.

Potential [%]	Temperature [° C]
0	25
25	51
50	82
75	115
100	150

For each test, the cold former operated for 10 minutes, while two samples, one after the cold forming process and the other after the thread rolling process were taken.

For each temperature the force needed for cold forming and for the thread rolling was noted. For the cold forming process, 5 different forces were detected, one for each of the five forming dies, and for the thread rolling process 2 forces, one in the front of the flat rolling die and one in the back, were measured. The measured forces in the tests with increasing temperatures can be viewed in Fig. 4-4.

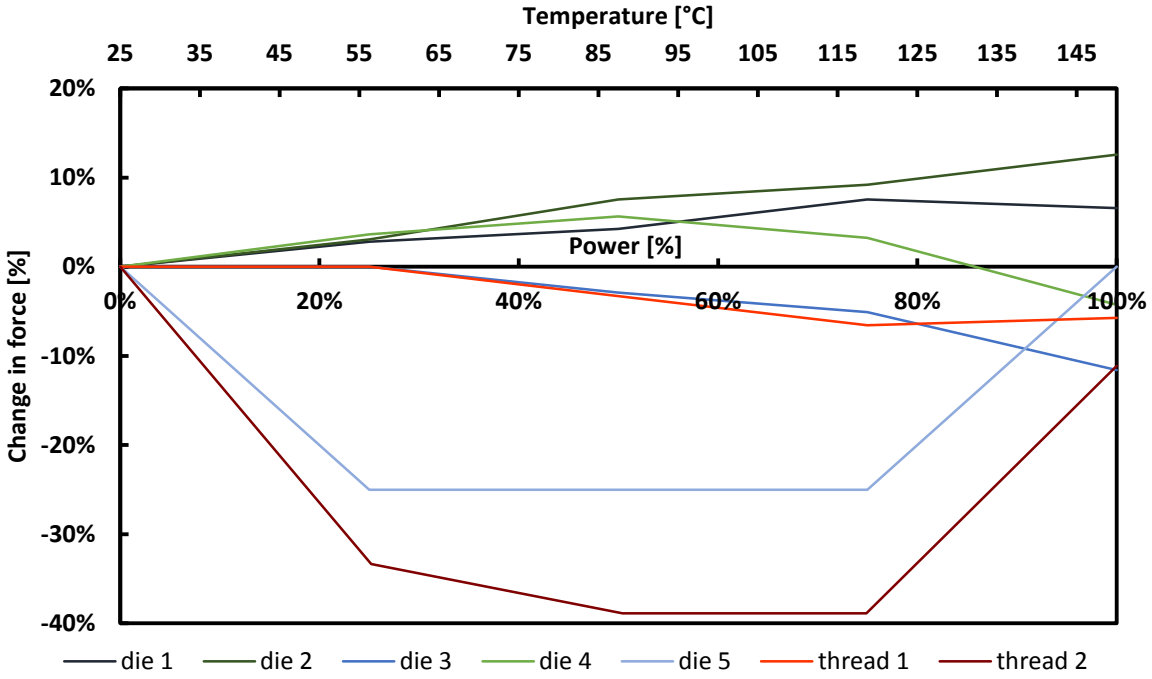

Fig. 4-4: Measured forces of the forming tests depending on the temperature.

On the basis of the diagram in Fig. 4-4 it seems, that the temperature has is general a positive influence on the force, as the bigger amounts of change in force are in the negative area. It can be seen, that the force, except of die 3 and die4, rises at to higher levels when the generator reaches 100% of its power. But the diagram does not show the fact, that not every die and every thread uses the same maximal force in the forming process. Therefore, Fig. 4-5 shows the influence of the power on the absolute force.

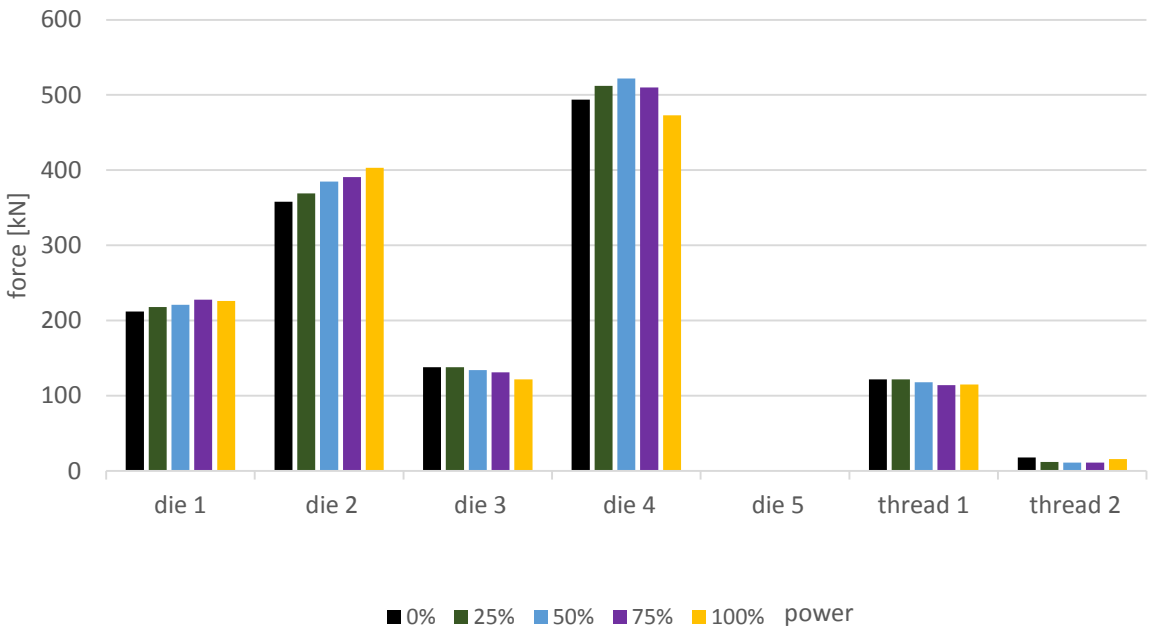

Fig. 4-5: Required forces of the different dies and threads at various powers.

As it can be clearly seen in Fig. 4-5 the forces of die 5 and thread 2 are too small to have a great impact on the whole system. Looking at Fig. 4-4 these two elements have relatively seen the biggest losses in force during the tests which leads to a false first impression. Elements like die 2 and die 4, which handle a very high load, do not show the expected load decrease. On the contrary, the force measured in die 2 rises up to 13 % from room temperature to 150° C.

Fig. 4-6 shows a summation of all forces used for the cold forming and thread rolling process for the tested temperatures. The force of the cold former rises from 1200 MPa at room temperature up to 1260 MPa at 82° C and 115° C which equals a rise in forces by 5 %. At 150° C the force decreases to 1225 MPa, a rise of 2 % from the force at room temperature. In comparison to the cold former, the thread roller decreases the overall force up to 11 % compared to its force at room temperature from 140 MPa. To 125 MPa at 115° C. At a temperature of 150° C a decrease in force to 130 MPa can be observed which equals loss of 6 % compared to the standard force at room temperature.

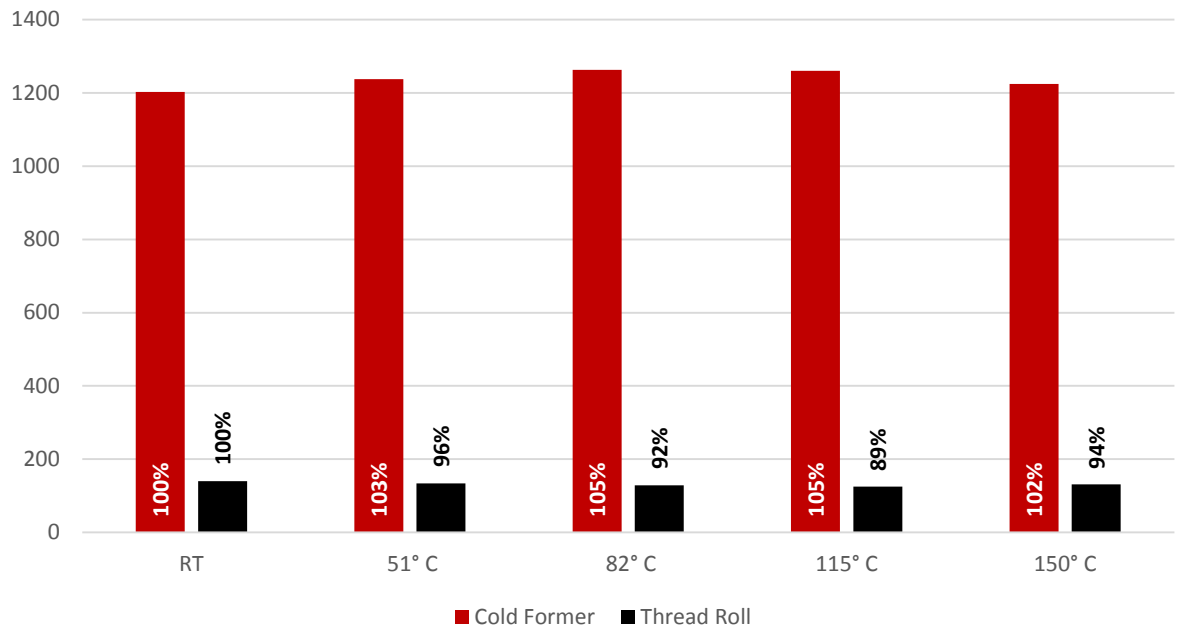

Fig. 4-6: Development of forces at different temperatures at the cold former (red) and the thread roll (black).

In order to determine the influence of preheating on the thread rolling process a thread rolled screw was measured on an optical measuring device every minute for a time period of 10 minutes. The major thread diameter increases and the minor thread diameter decreases in the start-up phase, defined as the first 10 minutes. This can be seen in Fig. 4-7 and Fig. 4-8. At a temperature of 150° C the test was stopped after 3 minutes because the drawn wire showed the first wear marks which would have led to a crash at the cold former. In order to do a proper analysis of the test results, the curve was later extrapolated up to 10 minutes.

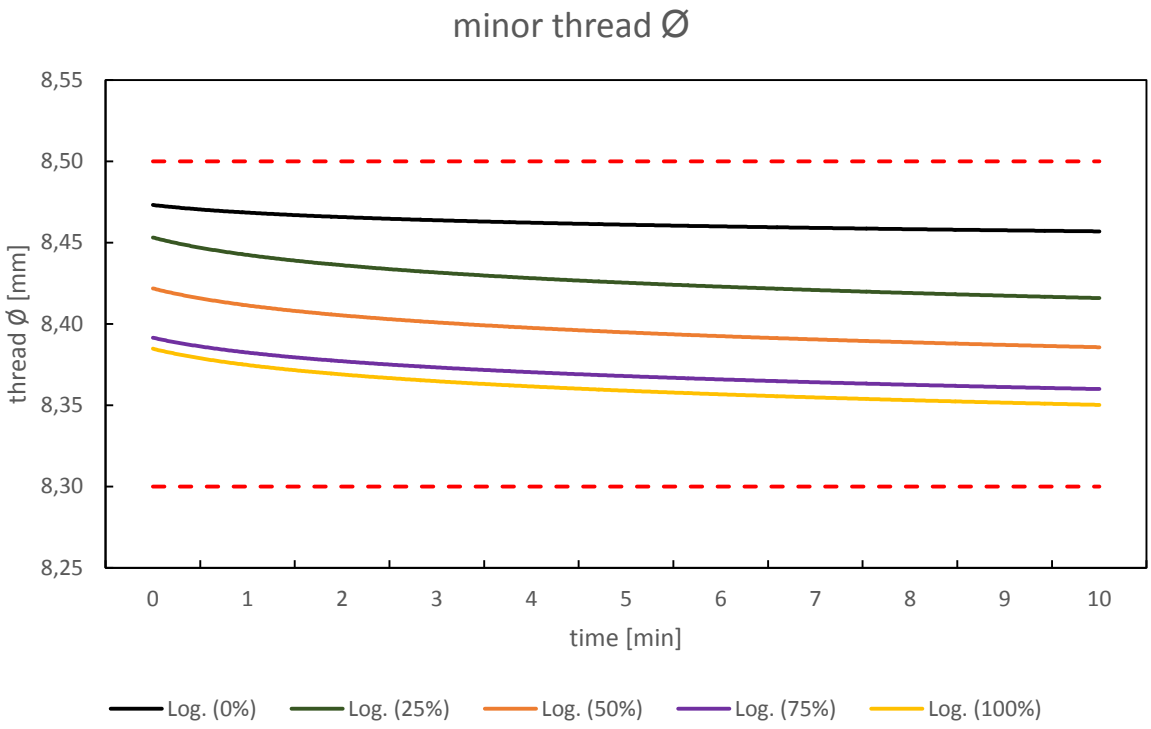

Fig. 4-7: Decrease of the minor thread diameter for different temperatures of the HUS-HR 10 due to better flow properties with rising temperatures at the start-up phase.

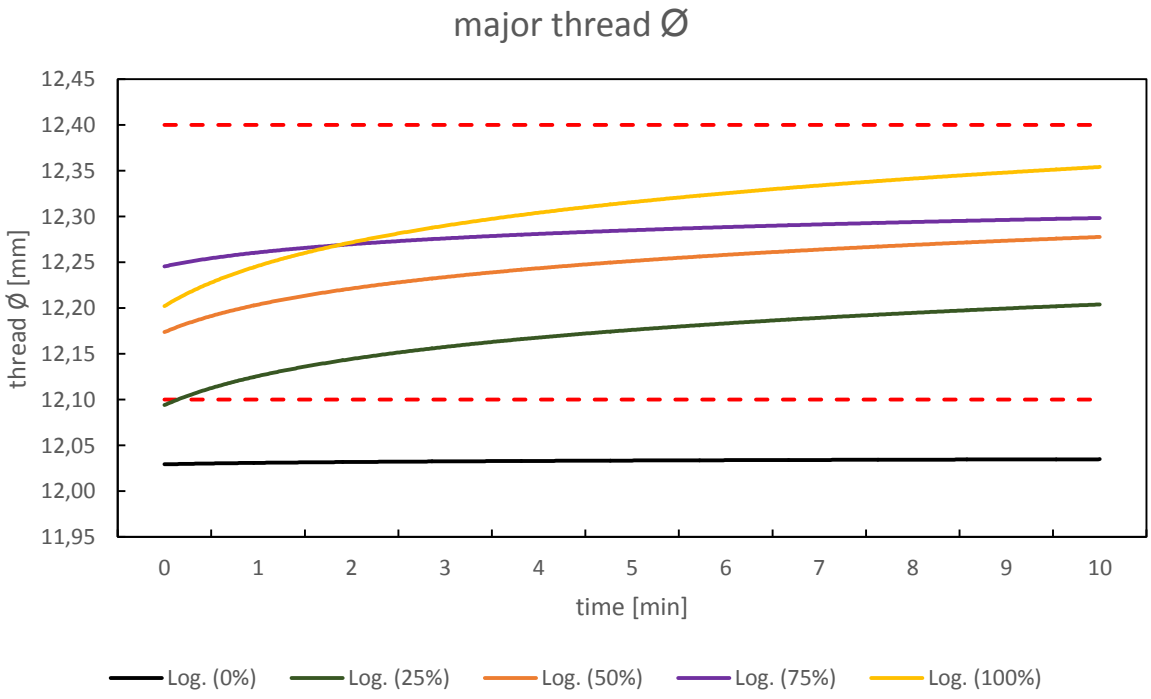

Fig. 4-8: Increase of the major thread diameter for different temperatures of the HUS-HR 10 due to better flow properties with rising temperatures at the start-up phase.

Important for the production is, that the maximum and minimum of the curve given by the increase or decrease of the diameter fits in the given tolerance field. Ideally the parameters at the start of the production are set on the upper tolerance limit for minor thread diameter and on the lower tolerance limit for the major thread diameter. In the course of the start-up phase, the change in diameter should be small enough, that it stays in between the tolerance limit. To observe the influence of the temperature on this matter, the diameter change respectively to the tolerance range is shown in Fig. 4-9 and Fig. 4-10.

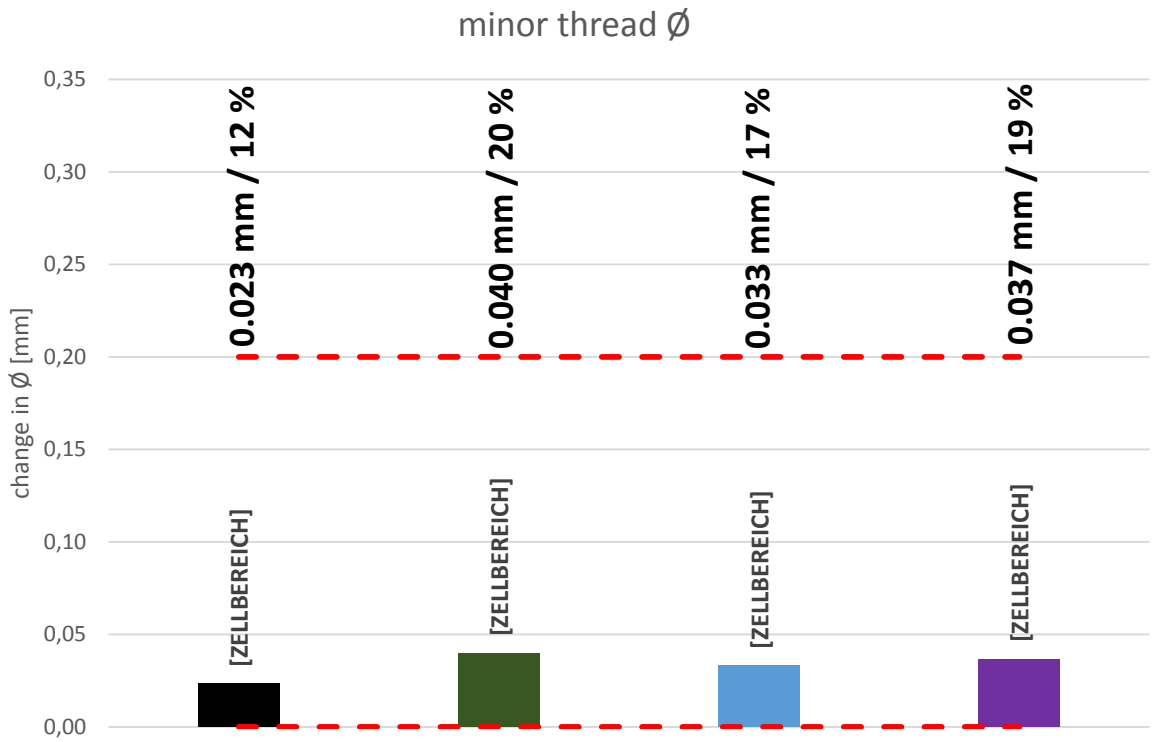

Fig. 4-9: Diameter change for the minor thread diameter in respect to the tolerance range.

The change in diameter for the minor thread over the time of the running-in period, which is the time the rolling dies need to reach operating temperature, is rather small compared to the defined tolerance range. Nevertheless, it seems do decrease with rising temperature. Starting with 0.02 mm of diameter decrease over the first 10 minutes of the production time which are 12 % compared to the tolerance range for the tests at room temperature it rises up to 20 % of the tolerance range with 0.04 mm for 51° C. For 115° C the diameter rises 0.037 % which are 19 % of the given tolerance range.

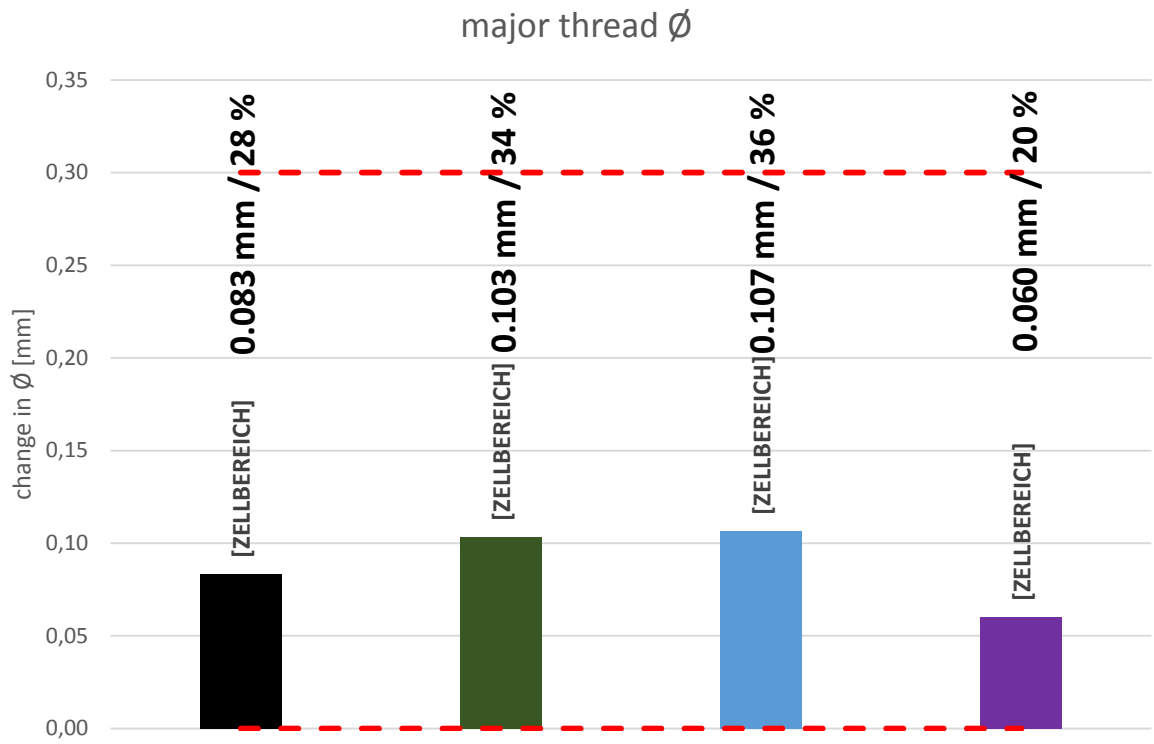

Fig. 4-10: Diameter change for the major thread diameter in respect to the tolerance range.

The change in diameter for the major thread diameter at room temperature is 0.08 mm which takes up 28 % of the tolerance range. With increasing temperatures, the diameter increases for 25 % and 50 % of the usable power and decrease at 100 % resulting in an enlargement of 0.06 mm for 115° C which is 20 % compared to the tolerance range.

4.2.3. Further attempts

Further attempts to reach higher temperatures also were not successful. Neither the power of the generator could be increased, nor the forming speed of the cold former could be decreased, because of software limitations. Also, the decrease of the diameter of the wire, testing on an HUS-HR 6 instead of the HUS-HR 10 used in all previous tests, did not lead to a temperature increase.

5. Discussion

5.1. Temperature-dependent yield strength

The gap between the results at the temperature-dependent yield strength tests can be mainly attributed to the fact, that the wire used for the Rastegaev samples, which were used for the tests at the Servotest TMTS and partly at the UPM Zwick & Roell “Zwick 1485”, has already been drawn at the cold former. The wire used for the standard samples, which were used at the first crush test at the UPM Zwick & Roell “Zwick 1485”, was not deformed wire. The process of wire drawing leads to work hardening of the material which can be seen in the plastic limit of the different curves in Fig. 5-1.

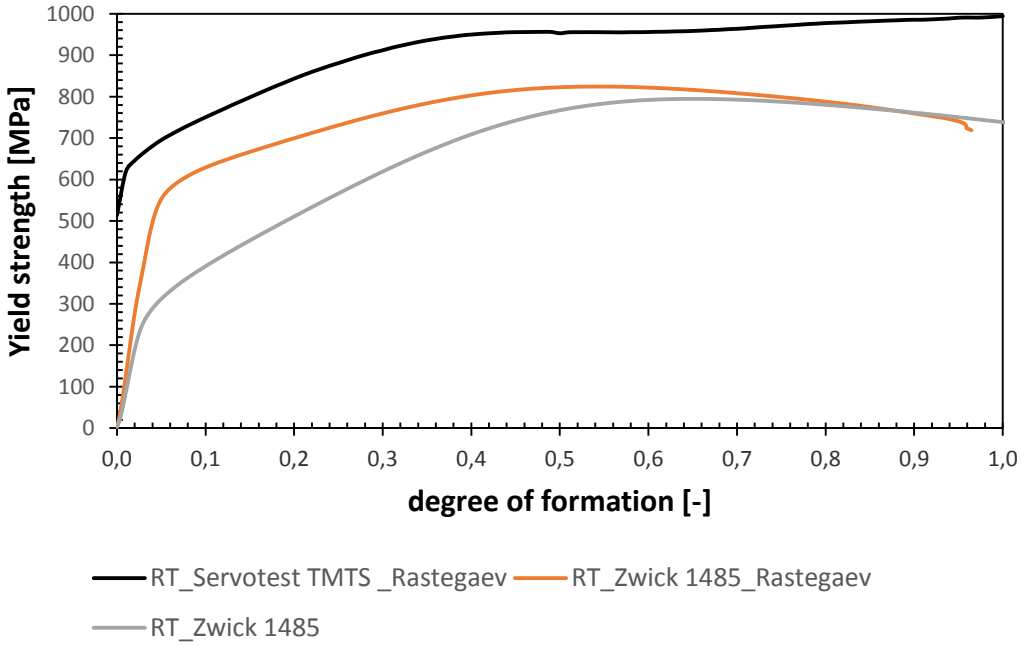

Fig. 5-1: Comparison of the three different tests at room temperature with two different samples at two different testing facilities.

Other influences may originate from the different forming speed, the different test device or the different sample geometry.

In order to get a better idea, why the gap between the curves at room temperature is this big, another test with on the one hand the standard samples, used for the tests at the UPM Zwick & Roell “Zwick 1485” before, and on the other hand Rastegaevsamples, which were used for the tests at the Servotest TMTS, were done at the UPM Zwick & Roell “Zwick 1485”.

The curve done with the Rastegaev samples shows a similar yield strength but different ultimate strength compared to the results of the Servotest TMTS, whereas the standard sample geometry and Rastegaev sample geometry show different Yield strengths but similar ultimate strength. This initiates an offset between the two testing machines and a major influence of drawn and not drawn wire.

Using the same sample geometry and testing machine, it is possible to give rough quantitative estimation of how a material would react in the forming process compared to other well-known materials tested with the same conditions. It also may help finding parameters for simulation processes.

The similarity of the results at 300° C and 350° C in Fig. 4-1 and Table 4.1 is most probably due the fact, that the heating process is not precise enough, which results in similar core temperatures near to 300° C. This is also reflected by the position of the curve in the diagram, which leads to a disproportionate big gap between the curve at 350° C and the curve at 400° C. These tests were performed at the UPM Zwick & Roell "Zwick 1485" using a chamber furnace which could lead to minor inaccuracies regarding the temperature.

The results of the crush test of the Servotest TMTS in comparison with those done at the Hilti AG show higher yield strengths for different temperatures. The maximal yield strength per tested temperature can be seen in Table 4.2. The maximal yield strength at room temperature is compared to the results at Hilit AG 200 MPa higher. The gap of the Yield strength between the two different tests is getting smaller, the higher the temperature gets as it can be seen in Table 5.1.

Table 5.1: Comparison between the Yield strengths of the two different tests.

Testing temperature	Maximal Yield strength UPM Zwick & Roell "Zwick 1485"	Maximal Yield strength Servotest TMTS
[° C]	[MPa]	[MPa]
20	795	994
50	-	937
100	-	871
150	-	795
200	662	734
250	627	712
300	599	672
350	600	656
400	550	593
450	-	570
500	-	560

5.2. Preheating

Because of the matter, that the used generator, Himmelwerk MU-25, had not enough power and the cold former is not able to run slower than 75 revolutions per minute it was not possible to heat the wire up to the initially planned 300° C. Therefore, it was not possible to get to a final evaluation of the process of wire preheating to 300° C before cold forming within this thesis. Nevertheless, it was possible to see a trend and first results leading to the development of a further experimental layout including different products and more powerful generators.

For the reached temperatures no decrease of the forming force could be observed whereas quite the contrary could be monitored. The force increased up to 5 % for the cold forming process. In order to get the full potential of the wire preheating process a change of the cold forming concept and the coating of the dies should be taken in consideration, as the whole process is designed for a pure cold forming process.

A temperature measurement of the screw after the fifth and last forming step during a standard forming process without preheating leaded to a temperature of around 200° C. A measurement of the temperature at the same position with preheating only leads up to 260° C. The high initial temperature resulting from the forming process could be another reason why 300° C could not decrease the force of the forming process.

As mentioned in 4.2.2 the rising temperature seems to have high influence on the flow properties of material and therefore on the diameter of the outer and inner thread. With higher temperature the outer diameter gets bigger and the lower diameter gets smaller. With this knowledge it may be possible to roll more complicated thread geometries by preheating.

6. Conclusion and Outlook

The motivation behind the preheating of wire for the cold forming process is to lower the production costs and open the possibilities to cold form more complex geometries. Looking at the results of the crush test the goal was to reach a temperature of 300° C and by that lower the forces by about 20 %.

As the results show, it is possible for a quantitative overview of the forming behaviour of a material to do crush tests at Hilti AG. But it is crucial, that a clear testing procedure is defined to avoid fluctuations in the testing results. It may be wise to favour a test setup where not drawn wire milled to Rastegaev samples are tested in a crush test. Strictly complying the testing setup ensures results which can be compared to the results of tested materials which are well known in the production and therefore it is possible to assess new materials and improve for example the results of a computer-aided simulation.

The conclusion of the preheating tests is that the used generator from the company Himmelwerk is not powerful enough to reach the desired temperature of 300° C. It was only possible to reach a temperature of 150° C with the given testing setup. It also should be taken in account, that the tests were carried out on the smallest length of the HUS-HR 10, for which the wire stays the longest in the inductor and therefore has the best conditions to get as hot as possible.

Considering all the experiences made in this thesis there are quite some things to be optimize for further tests. First, it is crucial to use a generator with more power. As a matter of fact, the used MU-25 is the weakest generator in its series. The company Himmelwerk recommended the use of the next generator in the list, which is the MU-40. Beside the more powerful generator there are some more things which have to be changed in order to optimize the results. A major influence on the heating process arises from the inductor. It is necessary to adapt the inner diameter from the inductor to the outer diameter of the ceramics tube so that the gap between the inductor and the coil is as small as possible. In order to get more time for heating the wire, the coil needs to be longer and maybe the windings have to be narrower. Another possibility for improvements is the optimization of the outer circle of the generator, the part on which the inductor is mounted. Several conductors can be changed or added to get the perfect setup for the given wire. With these

adaptations it will be possible to reach a temperature of 300° C and maybe get a positive impact on the forming force.

7. List of figures

8. List of tables

References

[1] J. Shields, C. Kovach, “Practical Guidelines for the Fabrication of High Performance Austenitic Stainless Steels.”, http://www.imoa.info/download_files/stainless-steel/Austenitics.pdf, January 2018.

[2] R. Schnitzer, J. Mayerhofer, “Vorlesung Werkstoffkunde der Stähle“, Montanuniversität Leoben, Leoben, 2017.

[3] H. Bhadeshia, R.W.K. Honeycombe, “Steels: Microstructure and Properties”, Elsevier, United Kingdom, 2017, p. 71 – 74.

[4] W.M. Garrison Jr., M.O.H. Amuda, “Stainless Steels: Martensitic”, Elsevier, United Kingdom, 2017, p. 5.

[5] C. Kittel, “Einführung in die Festkörperphysik”, R. Oldenbourg, München, 1996, p 15 – 46.

[6] H. M. Ledbetter, M. W. Austin, “Dilation of an fcc Fe-Cr-Ni alloy by interstitial carbon and nitrogen”, Material Science and Technology, vol. 3, no. 2, 1987, p. 101 – 104.

[7] D. Münter, “Struktur und Korrosionsverhalten nichtrostender Stähle nach einer chemisch-thermischen Behandlung bei tiefen Temperaturen, Dissertation, Fakultät für Werkstoffwissenschaften und Werkstofftechnologie“, Technische Universität Bergakademie Freiberg, Freiberg, 2009.

[8] M.G. Fontana, “Corrosion engineering“, McGraw-Hill Book Company, New York, 1987 p. 305 – 313.

[9] D. Dulieu, “The role of niobium in austenitic and duplex stainless steels”, Niobium 2001 Limited, Orlando, 2001, p. 975 – 1000.

[10] TMR Stainless AB, “Verarbeitung nichtrostender Duplexstähle – Ein praktischer Leitfaden. “, http://www.edelstahl-rostfrei.de/downloads/iser/Duplex_DE.pdf, January 2018.

[11] A.S. Khanna, “Introduction to High Temperature Oxidation and Corrosion”, ASM International, California,2011, p. 282 – 296.

[12] Outokumpu Stainless AB, “High Performance Austenitic Stainless Steel”, www.outokumpu-armetal.com/index.php?id=20, April 2018.

[13] M. Szala, K. Beer-Lech, M. Walczak, “A study on the corrosion of stainless steel floor drains in an indoor swimming pool”, Engineering Failure Analysis, vol. 77, 2017, p. 31 – 38.

[14] K. Sugimoto, Y. Sawada, “The role of molybdenum additions to austenitic stainless steels in the inhibition of pitting in acid chloride solution”, Corrosion Science, vol. 17, no. 5, 1977, p. 425 – 445.

[15] Y. Lang, H. Qu, H. Chen, Y. Weng, “Research Progress and Development Tendency of Nitrogen-alloyed Austenitic Stainless Steels”, International Journal of Iron and Steel Research, vol. 22, no. 2, 2015, p. 91 – 98.

[16] J. Zhu, R. Ding, J. He, Z. Yang, C. Yang, H. Chen, “A cyclic austenite reversion treatment for stabilizing austenite in the medium manganese steels”, Scripta Materialia, vol. 136, 2017, p. 6 – 10.

[17] E. Kunze, “Korrosion und Korrosionsschutz”, Wiley-VCH, Weinheim, 2009, p. 851 – 1075.

[18] B. Lv, F.C. Zhang, M. Li, R.J. Hou, L.H. Qian, T.S. Wang, “Effects of phosphorus and sulfur on the thermoplasticity of high manganese austenitic steel”, Materials Science and Engineering, vol. 527, no. 21, 2010, p. 5648 – 5653

[19] H. Clemens, “Vorlesung Metallkunde I”, Montanuniversität Leoben, Leoben, 2017.

[20] Nickel Development Institute, “Welding of stainless steel and other joining methods“, American Iron and Steel Institute, Washington DC, 1979, p. 8.

[21] N. Llorca-Isern, H. López-Luque, I. López-Jiménez, M.V. Biezma, “Identification of sigma and chi phases in duplex stainless steels”, Material Characterization, vol. 112, 2016, p. 20 – 29.

[22] B. Buchmayr, “Vorlesung Umformtechnik”, Montanuniversität Leoben, Leoben, 2016.

[23] K. Osakada, K. Mori, T. Altan, P. Groche, “Mechanical servo press technology for metal forming”, CIRP Annals, vol. 60, no.2, 2011, p. 651 – 672.

[24] S. Vaidya, P. Ambad, S. Bohsle, “Industry 4.0 – A Glimpse”, Procedia Manufacturing, vol. 20, 2018, p. 233 – 238.

[25] R.K. Mobley, “An Introduction to Predictive Maintenance (Second Edition)”, Butterworth-Heinemann Books, Burlington, 2002, p. 60.

[26] D. Goyal, B.S. Pabla, “Development of non-contact structural health monitoring system for machine tools”, Journal of Applied Research and Technology, vol. 14, no. 4, 2016, p. 245 – 258.

[27] Himmelwerk Hoch- und Mittelfrequenzanlagen GmbH, Serie MU 25 kW – 250 kW 8 kHz – 50 kHz, http://himmelwerk.com/produkte/baureihe-mu-ab-25kw, February 2018.

[28] M. Herrmann, F. Böhmermann, H. Hasselbruch, B. Kuhfuss, O. Riemer, A. Mehner, H.-W. Zoch, “Forming without Lubricant – Functionalized Tool Surface of Dry Forming Applications“, Procedia Manufacturing, vol. 8, 2017, p. 533 – 540.

[29] M. Brandt, “Laser Additive Manufacturing” Woodhead Publishing, Melbourne, 2017, p. 21 – 53.

[30] P. Köhnen, C. Haase, J. Bültmann, S. Ziegler, J.H. Schleifenbaum, W. Bleck, “Mechanical properties and deformation behaviour of additively manufactured lattice structures of stainless steel“, Materials & Design, vol. 145, 2018, p. 205 – 217.

[31] R. Meißner, M. Liewald, in Steels in Cars and Trucks 2017 Proceeding “Lightweight gearwheel design using separate gear ring and wheel body. Part II: Different manufacturing concepts for replacing a full body gearwheel”, Steel Institute VDEh, Düsseldorf, 2017, p. 1 – 2.

[32] W. Jaxa-Rozen, “Cold-worked austenitic stainless steels in passenger railcars and in other applications”, Thin-Walled Structures, vol. 83, 2014, p. 190 – 199.

[33] E.P. DeGarmo, J.T. Black, R.A. Kohser, “Materials and processes in manufacturing”, Wiley, New York, 2002, p. 159 – 173.

[34] G.E. Dieter, “Mechanical metallurgy”, McGraw-Hill, New York, 1961, p. 455 – 458.

[35] Nickel Development Institute, “Cold Forming Stainless Steel Bar and Wire“, https://www.nickelinstitute.org/~/media/Files/TechnicalLiterature/ColdFormingStainlessSteelBarandWire_9019_.ashx, January 2018.

[36] K.H.J Buschow, “Encyclopedia of materials” Science and Technology, Elsevier, Amsterdam, 2001, p. 5437 – 5439.

[37] Outokumpu Stainless AB, “Duplex, Austenitic-Ferritic stainless steel”, http://www.outokumpu.com/pages/SubAreaPage____45048.aspx, January 2018.

[38] C.V Nielsen, N. Bay, “Review of friction modelling in metal forming processes”, Journal of Materials Processing Technology, vol. 255, 2018, p. 234 – 241.

[39] N. Bay, A. Azushima, P. Groche, I. Ishibashi, M. Merklein, M. Morishita, T. Nakamura, S. Schmid, M. Yoshida, “Enviromental benign tribo-system for metal forming”, CIRP Annals, vol. 59, no. 2, 2010, p.760 – 780.

[40] K. Lange, M. Kammerer, K. Pöhlandt, J. Schöck, “Fließpressen – Wirtschaftliche Fertigung metallischer Präzisionswerkstücke“, Springer-Verlag, Berlin, 2008, p. 283 – 307.

[41] A.R. Lansdown, “Molybdenum Disulphide Lubrication“, Elsevier, United Kingdom, 1999, p. 380 – 412.

[42] W.J. Bartz, “Tribologie und Schmierung bei der Massivumformung“, expert verlag, Renningen-Malmsheim, 2004, p. 300 – 341.

[43] S.V. Raju, B.K. Godwal, J. Yan, R. Jeanloz, S.K. Saxena, “Yield strength of Ni-Al-Cr superalloy under pressure“, Journal of Alloys and Compounds, vol. 657, 2016, p. 889 – 892.

[44] M.F. McGuire, ”Stainless steels for design engineers”, ASM International, California , 2008, p. 69 – 91.

[45] S. Afshan, B. Rossi, L. Gardner, “Strength enhancements in cold-formed structural sections — Part I: Material testing”, Journal of Constructional Steel Research, vol. 83, 2013, p. 177 – 188.

[46] Valbruna, “Valbruna Werkstoffblatt MVAPML/1.4404”, https://www.valbruna.de/files/pdf/datenblatt_4404.pdf, January 2018.

[47] C.W. Kovach, “High-Performance Stainless Steels“, https://www.nickelinstitute.org/en/TechnicalLibrary/Reference%20Book%20Series/11021_HighPerformanceStainlessSteels.aspx, January 2018.

[48] Hilit Ag, “Screw anchor HUS-HR/CR (SS316)”, https://www.hilti.com/medias/sys_master/documents/hf8/he2/9270317613086/Technical-Supplement-for-HUS-HR-and-HUS-CR-Documentation-ASSET-DOC-LOC-7836263.pdf, February 2018.

[49] Deutsches Institut für Normung, “ DIN 50106:1978-12: Prüfung metallischer Werkstoffe – Druckversuch bei Raumtemperatur”, Beuth Verlag GmbH, Berlin , 2016, p. 2.

[50] E. Doege, H. Meyer-Nolkemper, I. Saeed, “Fließkurvenatlas metallischer Werkstoffe“, Hanser, München, 1986.